A quantitative analysis of cell volume and resting potential determination and regulation in excitable cells

James A. Fraser and Christopher L.-H. Huang

Physiological Laboratory, University of Cambridge, Downing Street, Cambridge CB2 3EG, UK

This paper quantifies recent experimental results through a general physical description of the mechanisms that might control two fundamental cellular parameters, resting potential (E_m) and cell volume (V_c), thereby clarifying the complex relationships between them. E_m was determined directly from a charge difference (CD) equation involving total intracellular ionic charge and membrane capacitance (C_m). This avoided the equilibrium condition $dE_m/dt = 0$ required in determinations of E_m by previous work based on the Goldman-Hodgkin-Katz equation and its derivatives and thus permitted precise calculation of E_m even under non-equilibrium conditions. It could accurately model the influence upon E_m of changes in C_m or V_c and of membrane transport processes such as the Na^+–K^+-ATPase and ion cotransport. Given a stable and adequate membrane Na^+–K^+-ATPase density (N), V_c and E_m both converged to unique steady-state values even from sharply divergent initial intracellular ionic concentrations. For any constant set of transmembrane ion permeabilities, this set point of V_c was then determined by the intracellular membrane-impermeant solute content (X^-_i) *and* its mean charge valency (z_X), while in contrast, the set point of E_m was determined *solely* by z_X. Independent changes in membrane Na^+ (P_{Na}) or K^+ permeabilities (P_K) or activation of cation–chloride cotransporters could perturb V_c and E_m but subsequent reversal of such changes permitted full recovery of both V_c and E_m to the original set points. *Proportionate* changes in P_{Na}, P_K and N, or changes in Cl^- permeability (P_{Cl}) instead conserved steady-state V_c and E_m but altered their *rates* of relaxation following any discrete perturbation. P_{Cl} additionally determined the relative effect of cotransporter activity on V_c and E_m, in agreement with recent experimental results. In contrast, changes in X_i^- produced by introduction of a finite permeability term to X^- (P_X) that did not alter z_X caused sustained changes in V_c that were independent of E_m and that persisted when P_X returned to zero. Where such fluxes also altered the effective z_X they additionally altered the steady state E_m. This offers a basis for the suggested roles of amino acid fluxes in long-term volume regulatory processes in a variety of excitable tissues.

(Received 2 April 2004; accepted after revision 2 July 2004; first published online 8 July 2004)
Corresponding author J. A. Fraser: Physiological Laboratory, University of Cambridge, Downing Street, Cambridge CB2 3EG, UK. Email: jaf21@cam.ac.uk

Cell volume (V_c) and resting potential (E_m) constitute two fundamental and interdependent baseline parameters important for cellular function. Adrian (1956) showed that membrane potentials of skeletal muscle fibres varied with extracellular osmolarity in solutions where K^+ constituted the only significant permeant ion. This E_m shift followed predicted alterations in relative intracellular and extracellular K^+ concentrations ($[K^+]_i$ and $[K^+]_e$) as expected if V_c varied linearly with reciprocal extracellular osmolarity (Dydynska & Wilkie, 1963; Blinks, 1965). However, more recent findings suggested a more complex relationship between V_c and E_m in more physiological extracellular solutions, and that this relationship diverged between different cell types. Ferenczi *et al.* (2004) suggested that osmotically induced shrinkage in skeletal muscle fibres activated inward Na^+–K^+–$2Cl^-$ cotransport (NKCC). This stabilized E_m despite expected increases in $[K^+]_i/[K^+]_e$ (Adrian, 1956), by holding $[Cl^-]_i/[Cl^-]_e$ above its equilibrium value (cf. Aickin *et al.* 1989). There was an accompanying trivial volume recovery in agreement with earlier work (Blinks, 1965). This behaviour contrasted sharply with that of several other cell types in which shrinkage-induced cotransporter activity produces marked regulatory volume increases

 DOI: 10.1113/jphysiol.2004.065706

(RVIs) (reviews: Lang *et al.* 1998*a*; O'Neill, 1999), but does not influence E_m (Lauf & Adragna, 2000). Similarly, while exhaustive exercise leads to increases in muscle fibre volume of up to 20% (Sjogaard *et al.* 1985), regulatory volume decrease (RVD) has never been demonstrated in mature skeletal muscle fibres (Sejersted & Sjogaard, 2000), although RVD is an almost ubiquitous response to swelling in non-excitable tissues (O'Neill, 1999; Okada *et al.* 2001). Yet long-term muscle fibre volumes *in vivo* remain remarkably stable (review: Proske & Morgan, 2001) despite this apparent regulation of E_m in preference to V_c in the short term (Ferenczi *et al.* 2004).

The present study reconciled and clarified these findings through the introduction of a mathematical model that incorporated the principal factors known to influence V_c and E_m. This interrelationship between V_c and E_m is of potential importance particularly in excitable cells: E_m depends on intracellular ion concentrations that are altered both by volume changes and by volume regulatory mechanisms. Skeletal muscle was used as a paradigm of excitable cells in view of recently recognized interactions between V_c and E_m in this tissue (Geukes Foppen *et al.* 2002; Ferenczi *et al.* 2004; Geukes Foppen, 2004). This study examined how cellular volume and resting potential might be determined, maintained and regulated by the wide range of interdependent membrane transport systems in excitable cells.

The model was designed to permit direct and precise calculation of E_m for any value of its rate of change, dE_m/dt. Therefore E_m was calculated directly from the membrane capacitance C_m and the intracellular charge difference, defined by the precise difference between the total charge carried by the positive and negative ions within the cell. This can be summarized in a charge difference (CD) equation:

$$E_m = \{F([Na^+]_i + [K^+]_i - [Cl^-]_i + z_X[X^-]_i)\}/C_m,$$

where $[X^-]_i$ denotes the internally sequestered osmolyte concentration and z_X its mean charge valency. Using this formulation, it was possible to calculate E_m precisely even under conditions where volume changes and/or volume regulatory mechanisms shifted transmembrane ion gradients away from electrochemical equilibrium, resulting in net transmembrane ion currents. Such currents would have violated the central assumption of earlier analyses that employed the Goldman-Hodgkin-Katz (GHK) equation (Goldman, 1943; Hodgkin & Katz, 1949), or derivatives such as the Mullins-Noda (MN) equation (Mullins & Noda, 1963) and the recent formulation of Armstrong (2003), which required $dE_m/dt = 0$.

Successive iterations using the charge difference method could calculate the effect upon E_m of any combination of quantitatively defined membrane transport processes after each suitably small time step of their activity. For example, the calculations incorporated a Na^+–K^+-ATPase model (Hernandez & Chifflet, 2000) and could simulate the electrogenic effect of this pump directly from the changing intracellular ion concentrations, without assuming the condition that $dE_m/dt = 0$, which is required for inclusion of an electrogenic sodium pump term in GHK-derivative equations (e.g. Mullins & Noda, 1963; Armstrong, 2003). This study additionally incorporated passive E_m-dependent ion fluxes (Goldman, 1943), membrane capacitance changes (Huang, 1981*a*,*b*), cation–chloride cotransport (Lauf & Adragna, 2000), non-monovalent organic anion fluxes (review: Strange *et al.* 1996), changes to z_X such as may occur when organic anions buffer pH changes, and volume changes and the consequent concentration or dilution of intracellular ions. This formulation could also be used to model ion antiport, rectifying and other non-linear permeabilities, voltage-gated ion channels, and the influence of imposed voltage steps upon V_c. Many of these processes would be difficult or perhaps impossible to model accurately using a GHK-based formulation.

Finally, flexibility in the iteration time step would permit modelling over any rate of change in any of the parameters (e.g. even during action potentials), in direct contrast to the central requirement of models based on the GHK equation that $dE_m/dt = 0$. Thus, comparison of the CD equation and the MN equation showed small but demonstrably significant discrepancies in calculated E_m when $dE_m/dt \neq 0$. However, when $dE_m/dt = 0$, substitution of the solute concentrations that were determined by the CD approach into the MN equation gave *steady state* E_m values in *perfect* agreement with the CD modelling, providing important confirmation of the validity of the charge-difference approach.

This study first demonstrated that V_c and E_m each converge to unique steady state values thereby offering fixed set points even in the absence of any specific cellular mechanisms sensing V_c or E_m. Secondly, the set point of V_c at constant extracellular osmolarity was determined *entirely* by the internally sequestered solute content (X_i) and its charge (z_X), given stable ion permeabilities and Na^+–K^+-ATPase density sufficient to maintain a stable volume. Thirdly, steady-state E_m under such conditions was determined solely by z_X, and relaxed to this value following any changes to intracellular inorganic ion concentrations or membrane capacitance. Fourthly, discrete changes in ion permeabilities, cotransport activity, Na^+–K^+-ATPase density, or extracellular osmolarity were shown to influence V_c and/or E_m. However, whatever the magnitude of the resulting perturbations, they completely reversed with reversal of the underlying changes without any requirement for specific V_c- or E_m-sensitive control mechanisms.

Finally, changes in V_c that in contrast were both sustained and independent of E_m occurred only with changes in cellular X^-_i content. Where such changes were simulated by the introduction of a finite permeability term to X^- (P_X), the resulting transmembrane effluxes of organic anion then produced sustained V_c decreases that persisted when P_X was returned to zero and *did not influence the set-point of* E_m. This might offer a basis for the possible role of amino acid fluxes in volume regulatory processes in a variety of excitable tissues, including cardiac muscle (Rasmusson *et al.* 1993), barnacle muscle (Pena-Rasgado *et al.* 2001) and hippocampal neurones (Pasantes-Morales *et al.* 2000; Olson *et al.* 2003). In contrast, fluxes that resulted in a change in effective z_X also altered the E_m set point. This might occur, for example, if an efflux consisted only of uncharged X, thus altering the mean charge on the remaining X_i. The model thus confirmed that organic osmolyte fluxes are entirely feasible for long-term volume regulation without necessarily disrupting E_m, and thus seem the most likely candidate for volume regulation in skeletal muscle, a cell type in which high P_{Cl} has been shown to prevent cation–chloride cotransport mechanisms for this purpose (Ferenczi *et al.* 2004). Furthermore, such changes to organic anion content appear to be both necessary and sufficient to produce volume changes of sufficient magnitude and permanence to underlie processes such as growth, atrophy and hypertrophy.

Mathematical model

The numerical model specifically avoided any dependence on the assumption of electrochemical equilibrium that was necessitated by earlier calculations of the membrane potential, E_m, using the Goldman-Hodgkin-Katz (GHK) equation or its derivatives (Mullins & Noda, 1963; Armstrong, 2003). Thus E_m was calculated at each iteration time point, t, from the difference between the sums of the intracellular positive and negative charges, i.e.

$$E_{m(t)} = \frac{F([K^+]_i + [Na^+]_i - [Cl^-]_i + z_X[X^-]_i)}{C_m} \quad (1)$$

F is Faraday's constant (C mol^{-1}), C_m (C V^{-1} l^{-1}) is the membrane capacitance referred to unit cell volume, $[X^-]_i$ represents the total concentration (M) of a variety of osmotically active and normally membrane impermeant cellular constituents that include cytosolic proteins, amino acids, nucleotides and phosphorus-containing anions (Maughan & Recchia, 1985; Maughan & Godt, 2001) and z_X (dimensionless) is the mean charge valency of X^-. z_X is negative; thus $[X^-]_i$ balances the charge of the high intracellular cation concentrations. Note that this equation implicitly assigns the charge valencies of K^+, Na^+ and Cl^- as $+1$, $+1$ and -1, respectively.

The passive ion fluxes were then modelled based on their electrochemical potentials, using the Goldman equations as modified by Hodgkin and Katz (Goldman, 1943; Hodgkin & Katz, 1949), such that for any solute S its flux (J_S) per cm^2 of cell membrane (mol cm^{-2} s^{-1}) is given by:

$$J_S = P_S\varepsilon_m([S]_e e^{(-\varphi)} - [S]_i e^{(\varphi)}) \quad (2)$$

where:

$$\varphi = \frac{z_S F E_m}{2RT} \text{ (dimensionless)},$$

$$\varepsilon_m = \frac{2\varphi}{(e^{\varphi} - e^{-\varphi})} \text{ (dimensionless)},$$

P_S (cm s^{-1}) is the permeability of the membrane to S, $[S]_e$ and $[S]_i$ the extracellular and intracellular concentrations of S (M), respectively, z_S (dimensionless) the charge valency of S, and F, R and T have their usual meanings. Note that fluxes of X^- could be simulated using this formulation, although unless otherwise stated, $P_X = 0$.

Na^+–K^+-ATPase activity was described by the detailed kinetic model reported by Hernandez *et al.* (1989) using rate constants and other numerical parameters as presented in Hernandez & Chifflet (2000). This employs a six-stage sequential kinetic model of sodium pump activity and calculates the pump flux J_P (mol cm^{-2} s^{-1}) as:

$$J_P = \frac{1}{\Sigma} N(\alpha - \beta) \quad (3)$$

where α is the product of six 'forward' rate constants, β the product of six 'reverse' rate constants, N the sodium pump density, and Σ is a function of all the rate constants and ligand concentrations, explicitly described in Hernandez *et al.* (1989). Therefore the outward sodium flux is $3J_P$ and the inward potassium flux is $2J_P$. The rate constants α and β depend on the following concentrations: $[ATP]_i$, $[ADP]_i$, [inorganic phosphate] ($[P_i]_i$), $[K^+]_i^2$, $[K^+]_e^2$, $[Na^+]_i^3$, $[Na^+]_e^3$ and E_m, as described in detail in the original papers (Hernandez *et al.* 1989; Hernandez & Chifflet, 2000) and not reproduced in full here. Hernandez & Chifflet's model effectively indicates that J_P depends on the free energy changes inherent in each pump cycle: thus J_P increases if the free energy change of each pump cycle becomes more favourable, for example if the transmembrane Na^+, K^+ or E_m gradients are reduced, or if the reaction ATP $\rightarrow$ ADP + P_i becomes more favourable (e.g. by an increase in $[ATP]_i$). Such dependence of J_P upon free energy changes has been explicitly demonstrated in cardiac muscle (Jansen *et al.* 2003). No further regulatory properties were added to this Na^+–K^+-ATPase activity.

The model also included contributions of the following cation–chloride cotransporters to transmembrane ion movements: the Na^+–K^+–$2Cl^-$ cotransporter (NKCC) and the K^+–Cl^- cotransporter (KCC). As the purpose of the study was to investigate the maximum possible

contributions of these ion transport mechanisms, no regulatory processes were modelled over and above any dependence of the fluxes upon the intracellular and extracellular concentrations of their transported ions. These fluxes were modelled based on arbitrary permeability terms, P_{NKCC} and P_{KCC} (dimensionless) expressed relative to the membrane permeability of potassium. The ion fluxes through these cotransporters were then calculated from the product of the transported species' transmembrane concentration gradients. Note that ion fluxes through the cotransporters were therefore independent of E_m, in agreement with experimental evidence (Lauf & Adragna, 2000). Thus:

$$J_{KCC} = P_K P_{KCC}([K^+]_e[Cl^-]_e - [K^+]_i[Cl^-]_i) \quad (4a)$$

$$J_{NKCC} = P_k P_{NKCC}([Na^+]_e[K^+]_e[Ci^-]_e^2 - [Na^+]_i[K^+]_i[Ci^-]_i^2) \quad (4b)$$

For example if $P_{NKCC} = 1$, $\{([Na^+]_e[K^+]_e[Cl^-]_e^2)/([Na^+]_i[K^+]_i[Cl^-]_i^2)\} = \{[K^+]_e/[K^+]_i\}$ and $E_m = 0$, then for every 1 mol flux of K^+ through background 'leak' channels, there would be a flux of 1 mol each of Na^+ and K^+, and 2 mol of Cl^- through the NKCC. However, as the transmembrane K^+ flux is dependent on E_m while fluxes through the NKCC are not, the 'permeability' terms of the cotransporters are not straightforwardly comparable to the basic ionic permeabilities at other values of E_m.

At this stage of calculation the net ionic fluxes were summed (expressed as J_{TOTAL} (M s^{-1}), positive inward), and water movement (volume change) calculated by assuming that all ion movements were accompanied by sufficient water to render the ion fluxes isosmotic to the extracellular medium. It is reasonable to assume water movement follows ion movement with no lag as cell permeability to water is at least 1000 times greater than to ions (Verkman, 1992; Frigeri *et al.* 2004). The relative volume after each time step was thus:

$$V_{c(t+1)} = V_{c(t)} \frac{(J_{TOTAL} A_m + \Pi_{i(t)})}{\Pi_e} \quad (5)$$

where A_m is the membrane area per unit volume (cm^2 l^{-1}) and Π_i and Π_e represent total intracellular and extracellular osmolarity, respectively (osmol l^{-1}). Note that A_m was maintained at a constant value that was independent of cell volume. Although it is likely that A_m would indeed vary with volume *in vivo*, this was not modelled for two reasons. Firstly, ionic permeability per unit membrane area and sodium pump density would be unlikely to stay constant if absolute membrane area changed. Secondly, while A_m does clearly influence the rate of transmembrane ion fluxes, it does not influence the relative rates of such fluxes. In other words, steady-state points of stability in the model are independent of the value of A_m. For a similar reason, average membrane permeabilities were used with the assumption that each cell was a tube of 75 μm diameter, giving $A_m = 5 \times 10^5$ cm^{-2} l^{-1}. No attempt was made to model the transverse tubular system separately, as this would influence the kinetics of the model, but not the final values of the modelled parameters.

During each iteration step the calculations were performed in the order of eqns (1)–(5). Then the new membrane potential ($E_{m(t+1)}$) was once again calculated from eqn (1) and the iteration cycles were repeated. The model was initiated with a step size of 10^{-8} s per iteration, and this step size was then dynamically adjusted with each iteration to maintain the rate of change of E_m at $< 10^{-6}$ V per iteration and the step size $< 10^{-3}$ s per iteration. The validity of this method was checked by repeating several of the simulations with step sizes fixed at much smaller or much larger step sizes (between 10^{-9} and 10^{-2} s per iteration). These preliminary simulations confirmed that, although excessively large step sizes could result in oscillation of the calculated E_m, if step size was small enough that such oscillations did not occur, step size had absolutely no effect on the overall rate of change of any parameter or on their final stable values. This step size above which oscillations would occur was dependant upon the rate of change of E_m, and thus limiting the rate of change of E_m in the variable step size model ensured such oscillations did not occur. Modelling based on the Mullins-Noda or Goldman-Hodgkin-Katz equation was performed with a fixed step size of 10^{-5} s per iteration. Each of these simulations was then repeated with a fixed step size of 10^{-4} s per iteration, and the results were identical in all cases.

Table 1 shows the standard parameters with which the modelling process was initiated, unless otherwise stated in the text. These parameters are representative of amphibian skeletal muscle, and are derived from a variety of sources. (Adrian, 1956; Eisenberg & Gage, 1969; Gage & Eisenberg, 1969; Maughan & Recchia, 1985; Hernandez *et al.* 1989; Huang & Peachey, 1989; Thompson & Fitts, 1992; Hernandez & Chifflet, 2000; Maughan & Godt, 2001; Clausen, 2003).

Results

I. Volume determination in a cell with constant membrane ion permeabilities, sodium pump density and extracellular osmolarity

The intrinsic properties of Na^+–K^+-ATPase activity ensure both attainment and maintenance of stable physiological values of E_m, V_c and intracellular solute concentrations. Animal cells normally maintain stable volumes (V_c), membrane potentials (E_m) and intracellular ion concentrations: such homeostasis ultimately requires a functioning Na^+–K^+-ATPase resulting in

Table 1. Symbols used in the text, and initial values of parameters used in the model

Parameter	Symbol	Value	Refs. (see legend)
Extracellular Na^+ concentration	$[Na^+]_e$	112.5 mM	1 (as frog Ringer)
Extracellular K^+ concentration	$[K^+]_e$	2.5 mM	1 (as frog Ringer)
Extracellular Cl^- concentration	$[Cl^-]_e$	115 mM	1 (as frog Ringer)
(Thus: Extracellular osmolarity)	Π_e	230 mosmol l^{-1}	1 (as frog Ringer)
Intracellular ATP concentration	$[ATP]_i$	6 mM	5, 7, 8
Intracellular ADP concentration	$[ADP]_i$	6×10^{-3} mM	5, 7, 8
Intracellular inorganic phosphate	$[P_i]_i$	4.95 mM	5, 7, 8
Membrane Na^+ permeability	P_{Na}	0.8×10^{-9} cm s^{-1}	1, 2
Membrane K^+ permeability	P_K	4×10^{-8} cm s^{-1}	1, 2
Membrane Cl^- permeability	P_{Cl}	1.2×10^{-7} cm s^{-1}	1, 2
(Thus: Ratio of permeabilities)	P_{Na}: P_K: P_{Cl}	0.02 : 1: 3	
Na^+–K^+-ATPase density	N	5×10^{-12} mol cm^{-2}	5, 8, 10
Mean organic osmolyte valency	z_X	− 1.6477	4, 9
Membrane capacitance	C_m	7 μF cm^{-2}	3, 6

Key to references: (1) Adrian (1956). (2) Eisenberg & Gage (1969). (3) Gage & Eisenberg (1969). (4) Maughan & Recchia (1985). (5) Hernandez *et al.* (1989). (6) Huang & Peachey (1989). (7) Thompson & Fitts (1992) (8) Hernandez & Chifflet (2000). (9) Maughan & Godt (2001). (10) Clausen (2003).

effective sodium pump activity, without which cells inevitably swell and eventually lyse due to an unopposed net ion influx (Tosteson & Hoffman, 1960). A first test of charge-difference (CD) modelling accordingly examined whether a model cell with basic parameters derived from experimental data (Table 1) successfully reproduced such pump-dependant stability. The results were contrasted with approaches using the alternative Goldman-Hodgkin-Katz (GHK) equation and its variants.

Figure 1 summarizes a simulation that used semi-arbitrarily chosen, as opposed to physiological, initial solute concentrations in order to avoid presupposing points of stability in the model: (to one decimal place) $[Na^+]_i = 126.7$ mM, $[K^+]_i = 2.5$ mM, $[Cl^-]_i = 57.5$ mM and $[X^-]_i = 43.5$ mM. These initial values, with the exception of the replacement of approximately half the Cl^- by organic anions (X^-), approximated normal *extra*cellular concentrations. Furthermore this particular choice of values gave a total initial intracellular charge difference of precisely zero, $E_{m(t=0)} = 0$ mV, by the CD method. Na^+–K^+-ATPase activity was left to be determined solely by its intrinsic dependences upon transported and energetic substrates, as described in the Mathematical model section, without any regulatory mechanisms involving any direct sensing of E_m or V_c.

E_m, V_c and each of the intracellular solute concentrations gradually approached stable final steady state values that strikingly reproduced the intracellular ion concentrations and E_m found in frog skeletal muscle (Hodgkin & Horowicz, 1959; Maughan & Recchia, 1985) despite such arbitrary starting parameters. The membrane potential $E_{m(MN)}$ was also calculated at each time point using the Mullins-Noda (MN) equation (Mullins & Noda, 1963) for comparison with the corresponding result $E_{m(CD)}$ from the charge difference equation. $E_{m(CD)}$ and the value of $E_{m(MN)}$ calculated from the values of the intracellular solute concentrations derived from CD modelling independently converged to identical *final* values (both precisely −88.235270 mV) despite the very different methods of calculation, particularly regarding the electrogenic sodium pump contribution. This strongly corroborates the validity of the CD modelling technique adopted here. However, $E_{m(MN)}$ was almost 1 mV less negative than $E_{m(CD)}$ in the initial transients. This may reflect the condition in the MN equation for calculation of resting membrane potential that requires perfectly balanced leak and electrogenic pump currents (Mullins & Noda, 1963). Similar requirements would apply to other analyses similarly based upon the Goldman-Hodgkin-Katz equation and its derivatives (see also Armstrong, 2003). The initial phase shown in Fig. 1 would generate significant net ionic fluxes that break this equilibrium assumption, result in $dE_m/dt \neq 0$ and consequently additionally require treatment of the capacitive current term $C_m(dE_m/dt)$.

However, at physiological resting ion permeabilities and values of Na^+–K^+-ATPase density (N), dE_m/dt appears relatively small even under disequilibrium conditions such as the starting conditions for Fig. 1. Accordingly, the significance of this early discrepancy between $E_{m(CD)}$ and $E_{m(MN)}$ was investigated. Alternative modelling, nevertheless using the same initial values as in Fig. 1, therefore calculated E_m at each step in the simulation from the MN rather than the CD equation (eqn (1)) such that E_m-dependant ion fluxes throughout the simulation (eqns (2) and (3)) were dependant upon $E_{m(MN)}$ rather

than $E_{m(CD)}$. This alternative model successfully reached stable final values of $[Na^+]_i$, $[K^+]_i$, $[Cl^-]_i$ and $[X^-]_i$ and E_m, but these values significantly differed from those obtained using the CD model: $[Na^+]_i = 17.6$ mM; $[K^+]_i = 105.6$ mM; $[Cl^-]_i = 4.3$ mM $[X^-]_i = 102.4$ mM; and $E_m = -84.7$ mV. These values appeared superficially reasonable; however, they produced a large charge discrepancy independent of the iteration time step employed such that;

$$\frac{F([K^+]_i + [Na^+]_i - [Cl^-]_i + z_X[X^-]_i)}{C_m} = -1718 \text{ V}.$$

Thus, in contrast to the convergence of $E_{m(MN)}$ with $E_{m(CD)}$ as $dE_m/dt \rightarrow 0$ in the CD equation model, these values instead diverged with each iteration that $dE_m/dt \neq 0$ in the otherwise identical MN equation model to reach impossible values. This emphasized the importance of precise modelling of E_m: transmembrane ion currents and E_m are interdependent values. In Fig. 1, where dE_m/dt is negative for each iteration until equilibrium is reached, $E_{m(MN)}$ is consistently slightly more positive than $E_{m(CD)}$. An example of the consequences of this is that outward K^+ flux is slightly increased over this period, amplifying the small discrepancies in E_m with each modelling step.

The recent formulation of Armstrong (2003) in which a sodium pump term was added to the GHK equation therefore shares its requirement that $dE_m/dt = 0$, and can additionally become insoluble due to a negative logarithmic term when active fluxes are significantly greater than passive fluxes. It was not therefore possible to repeat the above comparison with the model based on Armstrong's equation.

CD modelling demonstrates a convergence of V_c and E_m to unique steady-state values that are independent of the initial intracellular permeant ion concentrations and membrane capacitance. Figure 1 thus demonstrated that Na^+–K^+-ATPase activity alone, in the absence of any specific regulation towards predefined values of either E_m or V_c, inherently causes their convergence to stable final values from an arbitrary starting point. The following simulations investigated the factors that determine these absolute values of E_m, V_c and each intracellular solute concentration. First, Fig. 2 displays a simulation initiated from the final stable values from Fig. 1 apart from resetting V_c to 1. Complete inhibition of Na^+–K^+-ATPase activity after 20 min (marked with an asterisk) was followed as expected by the cell contents beginning gradually to equilibrate with the extracellular fluid. This was accompanied by a volume change that tracked the changing $[Cl^-]_i$ as might be expected in the absence of any other extracellular anions. However, Cl^- influx is not energetically favoured as Cl^- is normally passively distributed and thus at electrochemical equilibrium (possible effects of cation–chloride cotransport mechanisms are considered in section IV).

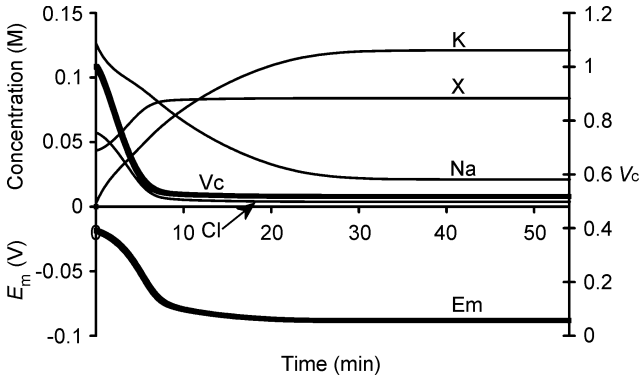

Figure 1. Activation of the sodium pump in a cell initially close to passive equilibrium
The model was initiated with values of all intracellular ionic concentrations close to equilibrium with the extracellular fluid, although with approximately half the normal organic anion concentration and a consequently lower $[Cl^-]_i$ to maintain a total intracellular charge difference of zero. Thus initially $[Na^+]_i = 126.7$ mM, $[K^+]_i = 2.5$ mM, $[Cl^-]_i = 57.5$ mM and $[X^-]_i = 43.5$ mM. V_c was initially defined as 1. Symbols are as follows: K: $[K^+]_i$; Na: $[Na^+]_i$; Cl: $[Cl^-]_i$; X: $[X^-]_i$; Em: E_m, Vc: V_c. The basic parameters such as ion permeabilities and sodium pump density were derived from frog skeletal muscle (Table 1). Note that despite the arbitrary starting conditions, each intracellular ion concentration, V_c and E_m all reach stable values that are strikingly similar to normal values for frog skeletal muscle.

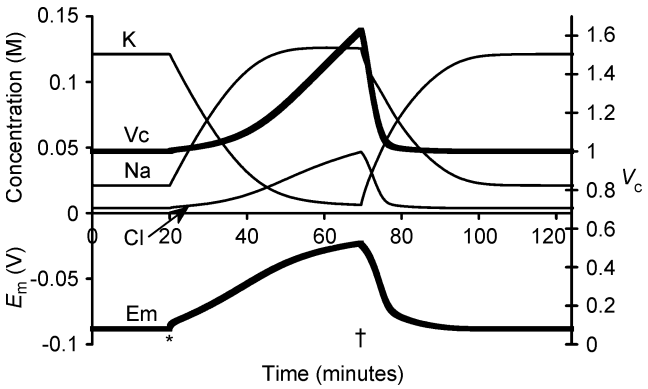

Figure 2. The effect of sodium pump inhibition
The model was initiated with variables derived from the final results shown in Fig. 1, and therefore all variables were initially stable. For clarity, $[X^-]_i$ is not shown, as it is membrane impermeant, and thus its concentration is straightforwardly related to V_c. At the point marked *, sodium pump density was reduced to zero, to simulate total sodium pump inhibition. Note the rapid small upward step in E_m that resulted from the loss of the electrogenic pump activity. Following this there was a gradual slower depolarization as $[K^+]_i$ and $[Na^+]_i$ began to equilibrate with the extracellular fluid. This depolarization allowed $[Cl^-]$ influx and thus volume increase. At the point marked †, sodium pump density was returned to its original value. Note that V_c, E_m and all intracellular ion concentrations returned to their starting values.

Nevertheless, it is apparent from Fig. 2 that the Cl^- entry could follow the depolarization of E_m, itself resulting primarily from the gradual reduction in $[K^+]_i$, as well as the loss of the small electrogenic contribution of the Na^+–K^+-ATPase. The time course of this cellular swelling was somewhat more rapid than has been observed in ouabain-treated skeletal muscle (e.g. Ferenczi *et al.* 2004), but closely agrees with previous attempts to model such phenomena (Hernandez & Cristina, 1998; Armstrong, 2003). Possible reasons for this apparent discrepancy are explored in section II below. Restoration of Na^+–K^+-ATPase activity 50 min later (marked with a dagger in Fig. 2) permitted recovery of each modelled variable to precisely its original value. Thus steady state V_c, E_m and all intracellular solute concentrations were all unchanged by a period without Na^+–K^+-ATPase activity despite the considerable perturbations that resulted.

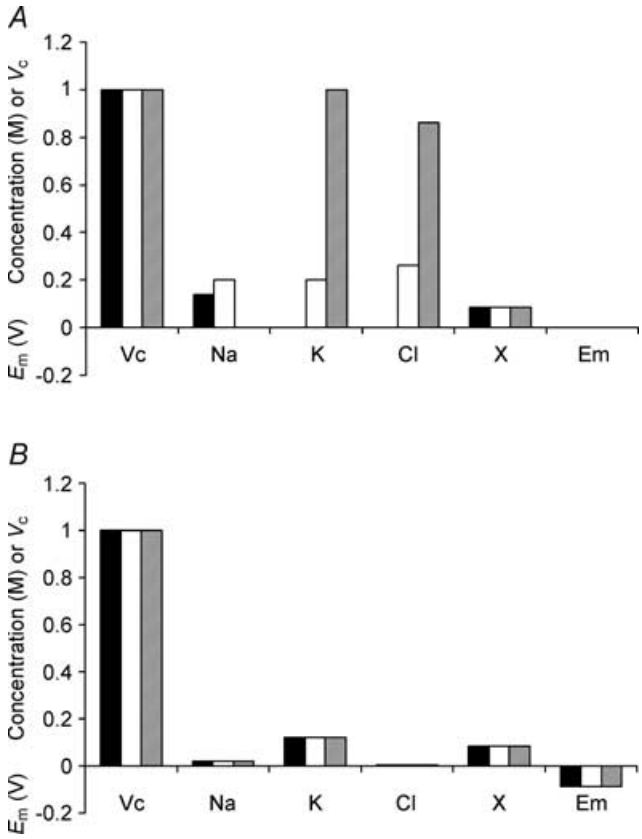

Figure 3. Initial intracellular inorganic ion concentrations do not influence eventual stable values of V_c or E_m
A, the starting conditions of three cells used as examples. The model was initiated with the intracellular organic anion concentration identical to that eventually reached in Fig. 1, but with three arbitrary and sharply different intracellular inorganic ion concentrations. Note that none of the cells were initially isotonic to the extracellular fluid. *B*, the final stable values reached after a 5-h modelling period. Variation in the initial intracellular inorganic ion concentrations has no influence on final stable values of V_c, E_m, $[Na^+]_i$, $[K^+]_i$, $[Cl^-]_i$ or $[X^-]_i$.

The second set of convergence tests used sharply contrasting initial intracellular concentrations of inorganic ions (Fig. 3*A*) but left $[X^-]_i$ identical to the final value shown in Fig. 1 and all other cellular parameters identical to those in Table 1. Figure 3*B* shows that corresponding final values of E_m, V_c, $[Na^+]_i$, $[K^+]_i$, $[Cl^-]_i$ and $[X^-]_i$ after a simulated 5 h period were entirely *independent* of these enormously divergent initial inorganic ion concentrations. Thus Cell 1 (filled column) began with [total intracellular osmolarity] < [extracellular osmolarity] and accordingly shrank in the initial stages of the simulation, concentrating all intracellular osmolytes. In sharp contrast, Cell 3 (grey column) began with a [total intracellular osmolarity] ≫ [extracellular osmolarity] and showed an initial swelling, which diluted all intracellular osmolytes. Nevertheless, both cells eventually equilibrated to exactly the same relative volumes and membrane potentials entirely independently of these initial intracellular ionic concentrations.

The possible influence of membrane capacitance (C_m) upon steady state value of E_m and V_c was also investigated, as C_m is known to vary significantly in skeletal muscle with changes in E_m even in the physiological range (Huang, 1981*a*,*b*). Figure 4 therefore shows the effects of large step changes in C_m in a simulation that was initiated with identical parameters to Fig. 2, although it should be noted

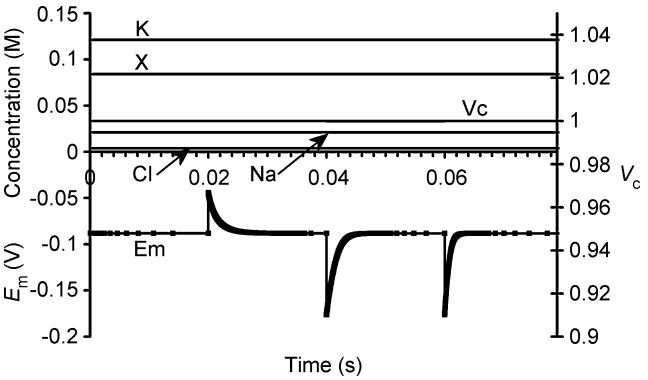

Figure 4. Membrane capacitance does not influence stable values of V_c or E_m
The model was initiated with variables derived from the final results shown in Fig. 1, and therefore all variables were initially stable. At 0.02 s, the membrane capacitance (C_m) was doubled from 7 μF cm^{-2} to 14 μF cm^{-2}. This caused an immediate halving of E_m, but E_m then relaxed towards its original value extremely rapidly (half-time 0.001 s). Although this reflected a submicromolar change in the charge difference, the ion concentrations and V_c were grossly unchanged. At 0.04 s, C_m was returned to 7 μF cm^{-2}, resulting in a reverse of the original step change in E_m and a similar relaxation toward resting values (half time 0.001 s). Finally at 0.06 s C_m was halved to 3.5 μF cm^{-2}, resulting in an immediate doubling of E_m, followed by its rapid relaxation towards the original steady state value (half-time 0.0005 s). Note the rapid time scale: E_m recovery to its steady state value following C_m changes occurs so rapidly that slow changes in C_m do not cause detectable E_m changes.

Table 2. A comparison of charge-difference-based modelling with Mullins-Noda equation-based modelling

E_m equation	Cell	V_c	$[Na^+]_i$ (M)	$[K^+]_i$ (M)	$[Cl^-]_i$ (M)	$[X^-]_i$ (M)	$E_{m(CD)}$ (V)	$E_{m(MN)}$ (V)	Π_i (M)
(Initial values)	1, $t = 0$	1	0.138	0.000	0.000	0.084	0	−0.09	0.222
	2, $t = 0$	1	0.200	0.200	0.262	0.084	0	+0.005	0.746
	3, $t = 0$	1	0.000	1.000	0.862	0.084	0	+0.002	1.946
CD	1, $t = \infty$	1	0.021	0.121	0.0038	0.084	−0.088	−0.088	0.230
CD	2, $t = \infty$	1	0.021	0.121	0.0038	0.084	−0.088	−0.088	0.230
CD	3, $t = \infty$	1	0.021	0.121	0.0038	0.084	−0.088	−0.088	0.230
MN	1, $t = \infty$	0.81	0.017	0.105	0.0044	0.103	**−1806**	−0.084	0.230
MN	2, $t = \infty$	1.12	0.023	0.129	0.0036	0.075	**+853**	−0.090	0.230
MN	3, $t = \infty$	2.4	0.034	0.158	0.0029	0.035	**+4509**	−0.095	0.230

The table shows $[Na^+]_i$, $[K^+]_i$, $[Cl^-]_i$, $[X^-]_i$ (V_c) and (E_m) for three cells with significantly different intracellular inorganic ion concentrations at $t = 0$, prior to modelling. The final stable values of each of these variables is shown for otherwise identical models based on either the charge-difference equation (CD) or the Mullins-Noda equation (MN) ($t = \infty$). Note that while the charge-difference model predicted that all three cells would stabilize with identical final values of each modelled variable, the Mullins-Noda model predicts final values that are dependant on the starting conditions. However, the Mullins-Noda model predicted final intracellular ion concentrations that were clearly impossible, as in each case there was a significant imbalance between the total concentrations of positive and negative ions within the cell (the magnitudes of the voltages suggested by these imbalances are shown in bold type). This resulted from the summation of many small errors in the calculation of E_m produced at each iteration step of the Mullins-Noda model for which dE_m/dt was not precisely zero, and hence E_m-dependant fluxes were consistently inaccurately modelled. In contrast, the Mullins-Noda equation is in perfect agreement with the charge-difference equation if the former is applied at the final point of stability of the charge difference model, where the assumption that $dE_m/dt = 0$ is entirely valid.

that the results are plotted against a much faster time base. As shown, each step change in C_m resulted in a reciprocal change in E_m, but E_m then relaxed rapidly towards its original resting value. When C_m was doubled from its normal value of 7 μF cm^{-2} to 14 μF cm^{-2} or when it was halved from 14 μF cm^{-2} to 7 μF cm^{-2} the half-time of the E_m recovery was 0.001 s. When C_m was halved from 7 μF cm^{-2} to 3.5 μF cm^{-2}, the half-time of E_m recovery was 0.0005 s. The half-time of relaxation of E_m therefore follows the expected relationship with changing C_m that it should be directly proportional to the magnitude of that change and therefore to the total resultant transmembrane charge movement. It is therefore apparent that even large changes in C_m do not influence steady state values of E_m. Furthermore, E_m correction to its steady state value following a change in C_m occurs so quickly that any changes in C_m that are considerably slower than those considered here (i.e. that take place over more than a few milliseconds) would not be expected to cause a detectable change in E_m. V_c and intracellular ion concentrations are grossly unaffected by changing C_m, although the E_m corrections to steady state values do of course reflect submicromolar readjustments in the *precise* ion concentrations from which the charge difference equation calculates E_m.

E_m, V_c and the concentrations of all intracellular solutes thus converge to fixed set points that are independent of other starting conditions given similar conditions of sodium pump density, ion permeabilities and intracellular impermeant organic anion content. This intrinsic regulatory property for baseline V_c and E_m does not require any existence of control processes explicitly sensitive to either V_c or E_m. E_m and V_c similarly return to exactly these unique stable values after any discrete perturbation to intracellular inorganic ion concentrations such as may occur during discrete periods of transmembrane cation–chloride cotransport (explicitly demonstrated in section IV).

Modelling based on the GHK equation fails to demonstrate unique V_c and E_m set points independent of initial intracellular inorganic ion concentrations. Table 2 demonstrates that simulations based upon the GHK equation and its derivatives yielded sharply divergent results. Although modelling using both the MN and the CD equations demonstrated that E_m, V_c and intracellular solute concentrations all converge to final stable values, only the CD model predicted that these final values were independent of the initial intracellular inorganic ion concentrations. By contrast, in the MN model these final values markedly depended upon the initial intracellular inorganic ion concentrations. Furthermore, use of the MN model predicted enormous discrepancies between the total intracellular concentrations of positive and negative ions that would predict impossibly high transmembrane voltages (shown in bold type). The contrasting predictions of the two forms of model were further examined using an analytic relationship between steady state V_c and E_m, for a cell with passive transmembrane distribution of

Cl^-, which is derived in the Appendix:

$$V_{c(t=\infty)} = \frac{(1 - z_X)[X^-]_{i(t=0)}}{\left(\Pi_e - 2[Cl^-]_e e^{(E_m F/RT)}\right)}$$

This formulation cannot be used to predict the steady state values of any of its variables but nevertheless usefully defines the *physically permissible* relationships between V_c, E_m, z_X, $[X^-]_i$, Π_e and $[Cl^-]$ by delimiting the range of values under which intracellular and extracellular osmolarity are equal, and the charge difference is small. It thus provided an important assay of the validity of the results from CD and MN modelling. The results in Table 2 from the CD model followed this relationship accurately. In contrast, the results from the MN model did not, further suggesting that the small inaccuracy in the calculated value of E_m under disequilibrium conditions was significant and that the precision of the CD model is an absolute requirement for accurate cellular modelling under such conditions. Furthermore, both the magnitudes and signs of these erroneous voltages themselves varied with the initial conditions. Using the basic GHK equation worsens these discrepancies (results not shown). These findings contrast sharply with charge difference-based modelling, which provides steady state values of E_m that are in *precise* agreement with the MN calculation based on the final concentrations derived from the CD model.

II. The effects of ion permeabilities and sodium pump density on cellular volume determination

Although the sodium pump is required to maintain V_c and E_m, variations in its activity within defined limits have little influence on their values in a stable cell. The demonstration that V_c and E_m converge to stable values that are independent of the initial intracellular inorganic ion concentrations prompted investigation of alternative factors that might determine these apparent set points. This began with an investigation of the relative importance of the sodium pump density (N) and transmembrane ion permeabilities in the determination of V_c and E_m. The simulation in Fig. 5*A* began from *after* a period in which the model was run from the final solute concentrations of Fig. 2 to its point of stability with an extremely high sodium pump density ($N = 10^{-7}$ mol cm^{-2}) (Else *et al.* 1996; Clausen, 2003). Thereafter, at each point marked with an asterisk, the sodium pump density was reduced 10-fold, and the model allowed to re-equilibrate. This process was repeated until the resultant pump rate could no longer maintain a stable cell volume as reflected in the relative magnitudes of the leakage currents and the maximum pump rate: the latter is achieved when $[Na^+]_i$ is at a maximum and E_m and $[K^+]_i$ are at a minimum. Figure 5*B* summarizes such effects of sodium pump density upon E_m and cell volume. Where $N <$ approximately 2×10^{-13} mol cm^{-2}, V_c and E_m did not reach stable values, and therefore V_c and E_m are plotted for $t = 50$ min (dashed line) and 150 min (continuous line) following a reduction in N to the lower value after a period of equilibration with $N = 5 \times 10^{-12}$ mol cm^{-2}.

Figure 5 thus demonstrates that even extremely large variations in N can leave E_m and V_c unchanged. In part this is a consequence of the fixed stoichiometry of the sodium pump, as this would imply that there is a point where the free energy output of hydrolysis of 1

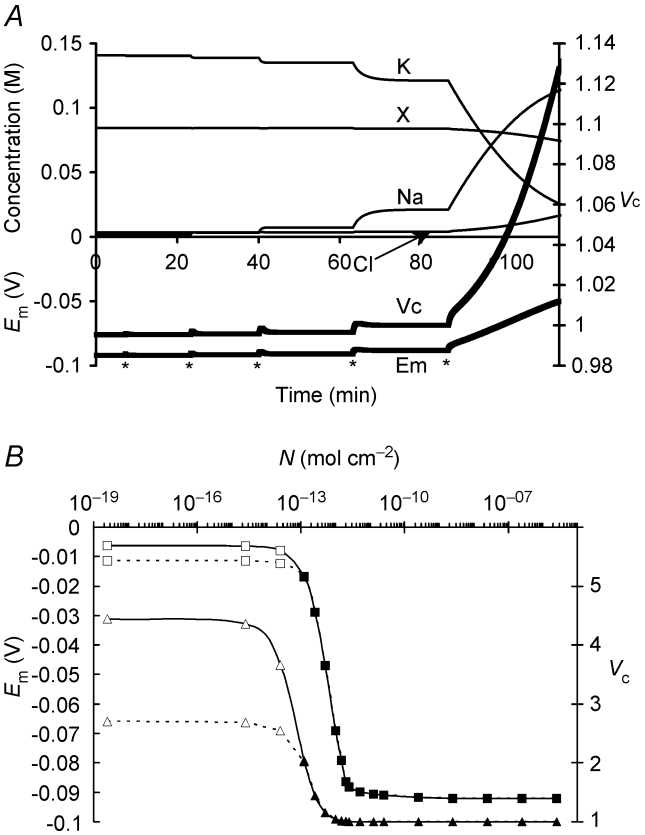

Figure 5. Sodium pump activity is required for volume stability, but within limits, variations in its activity leave V_c and E_m conserved

A, the effect of successive 10-fold reductions (each marked *) in sodium pump density (N) from an initial value of 5×10^{-8} mol cm^{-2}. Notice that at values of N sufficient to allow stable cell volume, large changes in N had relatively little effect on V_c or E_m, such that a 10 000-fold reduction to $N = 5 \times 10^{-12}$ mol cm^{-2} resulted in <1% increase in V_c and < 5% depolarization of E_m. However, a further 10-fold reduction in N destabilized cell volume. *B*, a summary of the relationship between N, V_c (triangles) and E_m (squares). Filled symbols denote final stable values, while for values of N insufficient to stabilize cell volume, the open symbols denote values of E_m or V_c obtained either 50 min (dashed line) or 150 min (continuous line) after N was reduced from 5×10^{-12} mol cm^{-2} to the value indicated. Note that, for this particular set of ion permeabilities, a pump density of at least 2.5×10^{-13} mol cm^{-2} was necessary for stability of V_c or E_m. Note that for all values of N sufficient to result in E_m of at least −80 mV ($N > 3 \times 10^{-12}$ mol cm^{-2}), variation in N has little influence on V_c or E_m. Thus for an excitable cell at least, variation of sodium pump density could not be expected to regulate or determine V_c or E_m.

molecule of ATP is insufficient to balance the free energy requirements of pumping 3 Na^+ and 2 K^+ against their respective electrochemical gradients. At this point, the sodium pump density becomes irrelevant. In excitable cells the electrochemical gradients are indeed extremely close to the point where activity of the Na^+–K^+-ATPase becomes energetically unfavourable (Jansen *et al.* 2003).

These findings suggest that if an excitable cell is to remain highly polarized, then while a sufficient level of sodium pump activity is clearly required to attain and maintain a stable volume, changes in its activity or density within such limits can have very little effect on V_c as sodium pump activity cannot influence V_c and E_m independently. Indeed, if N is the minimum sufficient to maintain E_m at less than −80 mV, then increasing it more than 1000-fold would decrease the cell volume by less than 2%. Conversely, although a small reduction in N from this point might result in significant swelling, this swelling would occur secondarily to a proportionately larger depolarization. Furthermore, such depolarization may result in a destabilization of cell volume due to Cl^- entry. In other words, such very low pump densities may be insufficient to *maintain* a stable cell volume, as maximum total pump activity may therefore be less than the resultant net leakage current. Finally, these properties arise simply from the intrinsic dependences of its sodium pump activity upon transported and energetic substrate in the absence of mechanisms that involve any direct sensing of V_c and E_m.

Transmembrane ion permeabilities influence E_m but cannot independently determine V_c. Figure 6*A* summarizes an investigation of how interactions between sodium pump density and transmembrane ion permeabilities influence V_c and E_m. Figure 6*Aa* explores the influence of the $P_{Na} : P_K$ ratio at constant P_K showing

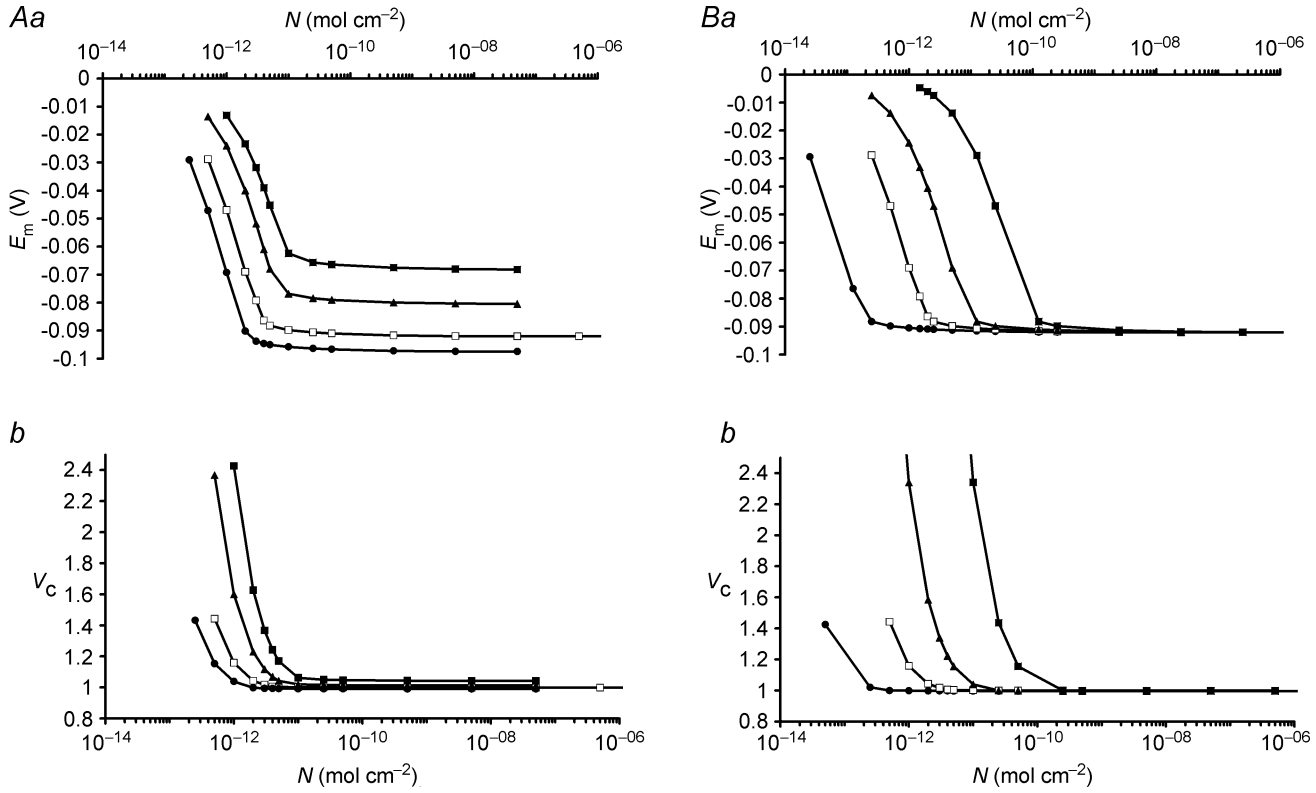

Figure 6. The influence of sodium and potassium permeabilities on V_c and E_m
In each figure, open symbols mark the line showing the relationship between N and V_c or E_m for the case of $P_{Na} : P_K = 0.02 : 1$, the permeability ratio explored in detail in Fig. 5. For clarity, only N-values that result in stable values of E_m and V_c are plotted in this figure. *A*, at constant P_K, the relationship between N and (*a*) E_m or *(b)* V_c for four different $P_K : P_{Na}$ ratios. $P_{Na} : P_K$ ratios: ● 0.01 : 1; □ 0.02 : 1; ▲ 0.05 : 1; ■ 0.1 : 1. *B*, at constant P_K/P_{Na}, the relationship between N and (*a*) E_m or *(b)* V_c for four different values of P_K. $P_{Na} : P_K$ ratios: ● 0.002 : 0.1; □ 0.02 : 1; ▲ 0.1 : 5; ■ 1 : 50. Note that increases in P_K without alteration of the $P_{Na} : P_K$ ratio resulted in a rightward shift of the E_m or V_c against N plots of equal magnitude, such that variation in P_K with a constant $P_{Na} : P_K : N$ ratio did not change E_m or V_c set point. In contrast, an increase of the $P_{Na} : P_K$ ratio at constant P_K resulted primarily in an upward shift of the E_m or V_c against N curves. P_{Cl} did not influence the steady state values of any of the modelled variables (not shown).

only values of N that result in stable values of E_m and V_c for clarity. Increasing the $P_{Na} : P_K$ ratio in isolation depolarizes E_m for all values of N and produces an upward shift of the E_m against N plot. It also increased the minimum value of N required to maintain a stable cell reflected in the additional rightward shift of the E_m against N plot. Figure 6*Ab*, shows that the change in E_m and the resultant change in $[Cl^-]_i$ shown in Fig. 6*Aa* secondarily influenced V_c.

In contrast Fig. 6*B* shows that increases in *both* P_{Na} and P_K in proportion simply produced a proportional rightward shift of the E_m or V_c against N curves, and therefore the original steady state set points of both V_c and E_m would be conserved provided the proportions $P_{Na} : P_K : N$ remained constant. Instead, any change in the magnitude of these values altered the kinetics with which E_m and V_c returned to their set values following any discrete perturbation. It may be noted that the rate of cell swelling following sodium pump inhibition shown in Fig. 2 would fit better with experimental observations (Ferenczi *et al.* 2004) were P_K rather lower than published values (Adrian, 1956) while maintaining the ratio $P_{Na} : P_K : N$.

Finally, all changes in P_{Cl} where $P_{Cl} > 0$ had no effect on the E_m or V_c set points where the transmembrane distribution of Cl^- was entirely passive, as its intracellular concentration, and hence V_c would then be determined entirely by the set point of E_m, which would be defined by the other factors discussed. However, P_{Cl} can influence the rate at which E_m and V_c return to their set points following, for example, cotransporter activation (see section IV).

III. The role of intracellular impermeant solute in cellular volume determination

Cellular volume is primarily determined by impermeant ion content and charge. The previous simulations clearly showed that sodium pump activity provides both a necessary and sufficient condition for attainment and maintenance of a stable V_c (Figs 1 and 2), that V_c is then determined independently of initial intracellular ion concentrations (Fig. 3) and membrane capacitance (Fig. 4), and that changes to sodium pump density (Fig. 5) or inorganic ion permeabilities (Fig. 6) within stable limits could have relatively little influence on V_c without a far greater effect on E_m. The simulations in Fig. 7 provide a contrasting demonstration that it is the intracellular impermeant anion content (modelled as a change in the ratio $[X^-]_i : \Pi_e$) that influences the set point of V_c, but that this has *no* influence on the set point of E_m. Note that initial charge neutrality, despite these variations in the initial value of $[X^-]_i$, was achieved by adjusting the initial concentrations of inorganic ions (Fig. 7*A*). Nevertheless Fig. 3 showed that the initial concentration of inorganic ions does not influence set points of either V_c or E_m. Figure 7*B* shows that, whereas alterations in the initial concentration of inorganic ions leaves V_c and E_m constant, changes in $[X^-]_{i(t=0)}$ altered the set point of V_c while leaving the corresponding set points of all other parameters, including E_m, unaffected. The simulation could be extended to the limit to demonstrate that intracellular impermeant anion is necessary to prevent the action of the sodium pump resulting in $V_c \rightarrow 0$.

As the impermeant anion, X^-_i, could potentially influence V_c and E_m through both its osmotic effect and its electrical charge, the model was next extended to clarify the effect of the mean charge valency of X^- (z_X). Once again initial concentrations of inorganic ions were appropriately corrected to maintain an initial charge difference of zero, but such changes do not influence the set points of V_c or E_m. Figure 8 summarizes the effect upon V_c of varying z_X at a fixed initial $[X]_i$ (Fig. 8*A*) using three values of $z_X = 2$ (filled column), 1 (open column)

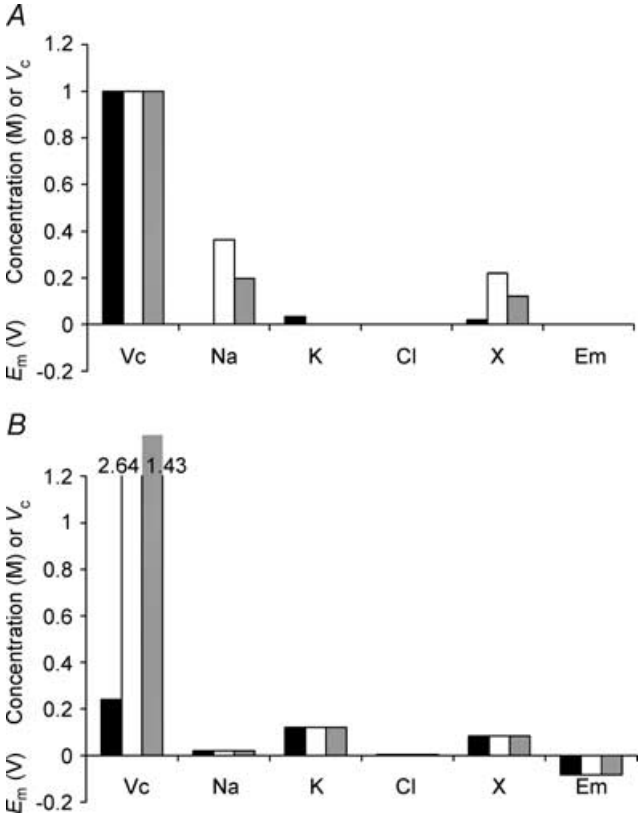

Figure 7. Intracellular organic ion concentration determines the eventual stable value of V_c but does not influence E_m
A, the starting conditions of three cells. These cells were modelled with initially different intracellular organic anion concentrations. Note that although initial intracellular inorganic ion concentrations also varied between the three cells, this would have no influence on the final stable values of V_c or E_m (see Fig. 3). *B*, the final stable values reached after a 5-h modelling period. Each cell reached identical stable values of E_m, $[Na^+]_i$, $[K^+]_i$, $[Cl^-]_i$ or $[X^-]_i$, demonstrating that variation of intracellular organic anion content has no influence on these variables. In contrast, the final stable volumes were sharply different.

and 0 (grey column), respectively. Figure 8*B* shows that the value of z_X influenced the set points of *all* modelled variables, including those of both V_c and E_m. Figure 8*C* summarizes the precise relationship between z_X, V_c and E_m and this shows that, for a given initial concentration of impermeant intracellular anion ($[X^-]_{i(t=0)}$), the set point of V_c is almost linearly related to z_X; the relationship is linear for higher magnitudes of z_X, while at lower magnitudes of z_X, the effect of the osmolarity of X^-_i has a proportionately greater influence. For $z_X \gg 0$, at physiological initial values of $[X^-]_i$ (approximately 85 mM), V_c is proportional to the magnitude of the valency with the approximate relationship $V_c = 0.37z_X + 0.39$ (a more general relationship is derived in the Appendix). This should be compared with the results of Fig. 3, in which it was shown that cells with identical $[X^-]_{i(t=0)}$ reach identical final values of V_c, E_m and all intracellular solute concentrations. Figure 8*C* thus shows that this conclusion is dependent upon z_X. Furthermore, it is probable that the value of z_X may change *in vivo*, for example in response to pH changes, and this could result in changes to steady state V_c, E_m and all intracellular solute concentrations.

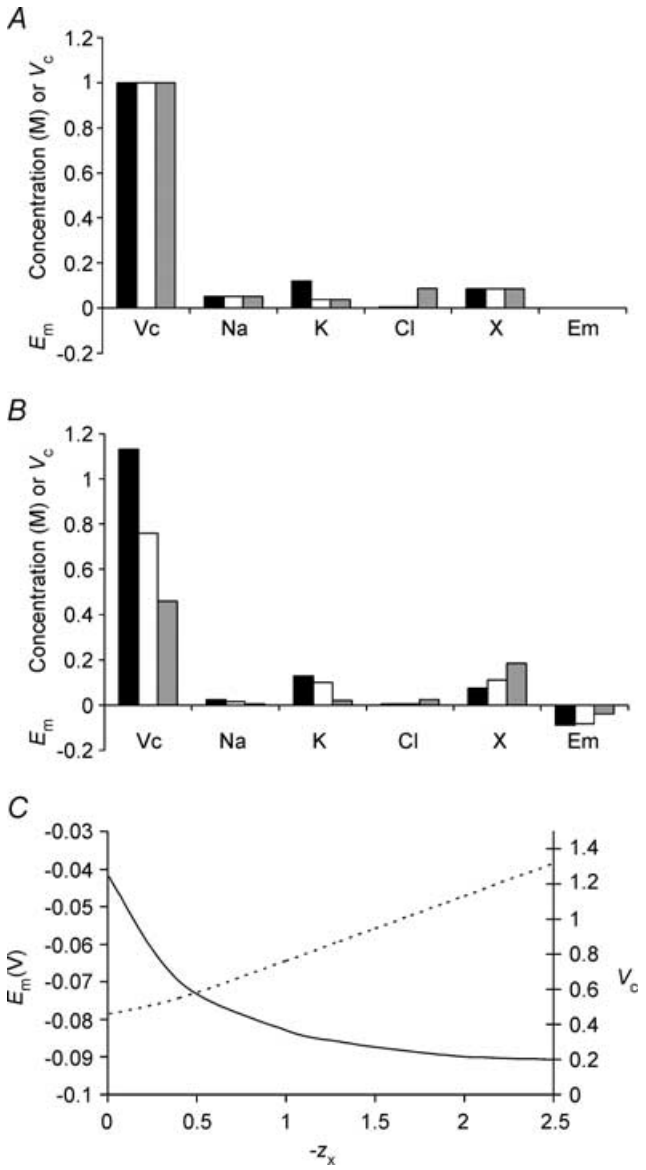

Figure 8. The mean valency of intracellular organic osmolyte influences the eventual stable values of both V_c and E_m
A, the starting conditions of three cells. These cells were modelled with initially identical intracellular organic osmolyte concentrations, but in each cell the mean charge valency of this osmolyte (z_X) was different. Note that although initial intracellular inorganic ion concentrations also varied between the three cells, this would have no influence on the final stable values of V_c or E_m (see Fig. 3). Filled columns: $z_X = 2$; open columns, $z_X = 1$; grey columns, $z_X = 0$. *B*, the final stable values reached after a 5- h modelling period. Each cell reached stable values of V_c, E_m, $[Na^+]_i$, $[K^+]_i$, $[Cl^-]_i$ or $[X^-]_i$, but there were no similarities between the three cells. Increasing the negative charge on intracellular organic osmolyte produced larger, more highly polarized cells. *C*, a summary of the influence of z_X upon E_m (continuous line) and V_c (dashed line).

One further finding was that lower magnitudes of z_X required fewer Na^+–K^+-ATPase cycles to maintain stable V_c and E_m, in a sense because reducing z_X reduces the tendency of the cell to swell. Although the maximum obtainable E_m is also reduced by this manipulation, it may be that non-excitable cells have lower z_X than excitable cells in order to conserve energy.

IV. Short-term *versus* long-term volume regulation

Cation–chloride cotransport permits short-term changes in V_c and/or E_m and such changes depend upon cellular Cl^- content and permeability. The simulations above show that cell volume is ultimately maintained by Na^+–K^+-ATPase activity, and when membrane ion permeabilities are constant, is determined primarily by the intracellular impermeant anion content and its charge. However, many cell-types exhibit RVI and RVD driven by transmembrane ion fluxes (reviews: Lang *et al.* 1998*a*,*b*). Furthermore, skeletal muscle is known to express at least the K^+–Cl^- cotransporter (KCC) (Lauf & Adragna, 2000) and the Na^+–K^+–$2Cl^-$ cotransporter (NKCC) (Wong *et al.* 1999; Lindinger *et al.* 2002). Together with the findings above (see, for example, Fig. 3) that V_c and E_m set points appear independent of intracellular ion concentrations, this prompted direct examination of the potential roles of the cation–chloride cotransporters in volume regulation.

Figure 9*A* shows the effect of a 40-min period of Na^+–K^+–$2Cl^-$ cotransporter (NKCC) activation in skeletal muscle. The value of P_{NKCC} was initially zero, was then increased to 10 000 at 20 min, and was finally returned to zero at 60 min. This transient activity had three main effects. First, NKCC activity resulted in an increase in V_c (∼20%) that was small in comparison to the significant depolarization of E_m (> 50%). This was because NKCC activity held $[Cl^-]_i/[Cl^-]_e$ above its normal electrochemical equilibrium, and due to the high P_{Cl} of skeletal muscle, this resulted in significant depolarization

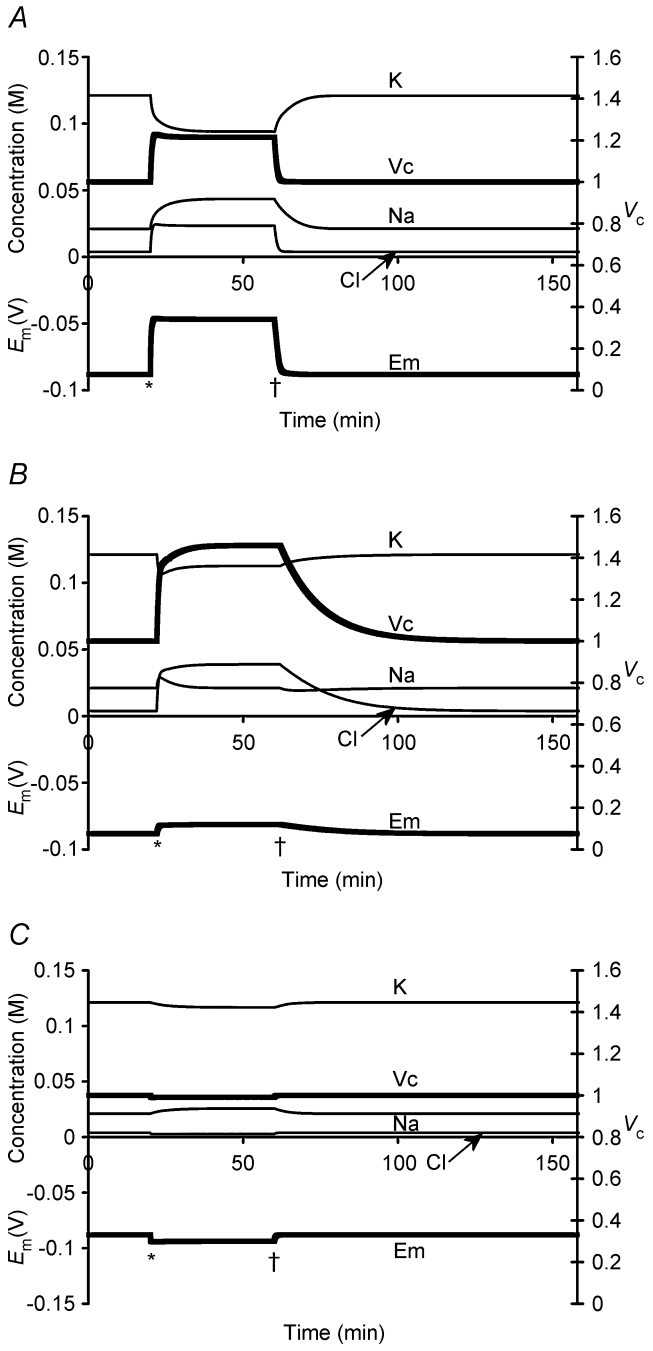

Figure 9. The effects of cation–chloride cotransport activity
NKCC activity in a tissue with $P_{Cl}/P_K = 3$ (similar to that of skeletal muscle) (*A*) and $P_{Cl}/P_K = 0.05$ (similar to that of an erythrocyte) (*B*). All other parameters were identical, and both cells were subjected to the same levels of NKCC activity. Thus in each case P_{NKCC} was initially 0, was stepped to 10 000 after 20 min (marked *), and was then returned to 0 at 60 min (marked †). Note that in each case, the NKCC caused a rapid increase in $[Na^+]_i$ and $[Cl^-]_i$, and a paradoxical reduction in $[K^+]_i$ despite an increase in cellular K^+ content, due to the concomitant water influx. In addition, both cells reached new stable values of V_c, E_m and all intracellular solute concentrations despite the continued ion influx through the NKCC. This was due to a reduction in NKCC activity as the $[Na^+]_i[K^+]_i[Cl^-]_i^2$ product increased, and an increase in Na^+–K^+-ATPase activity as the $[Na^+]_i$ increased, $[K^+]_i$ decreased and E_m depolarized. However, in the cell depicted in panel *A*, E_m depolarized very significantly (>50% reduction) while V_c increased by approximately 20%. In contrast, the cell depicted in panel *B* showed very significant swelling (>40%) and very little depolarization of E_m (<10%). The rate of recovery to normal values of E_m and V_c following cessation of NKCC activity is also significantly different between the two cells. *C*, corresponding effects of KCC activity in a high P_{Cl} cell. Although efflux of K^+ and Cl^- was initially favourable, the efflux was severely limited by the low $[Cl^-]_i$ in such a highly polarized cell. V_c therefore decreased by <1%, while E_m hyperpolarized by 5 mV. Note the small increase in $[Na^+]_i$ and decrease in $[K^+]_i$ due to the effect of this hyperpolarization upon the Na^+–K^+-ATPase.

of E_m. Secondly, sustained NKCC activation *did not* result in continued swelling or depolarization. Rather, it shifted V_c and E_m to new stable values. This new steady state reflected a gradual reduction in the rate of NKCC activity and a parallel increase in Na^+–K^+-ATPase activity. The decreased NKCC activity resulted from a gradual reduction in the initially favourable gradient for coupled Na^+, K^+ and 2 Cl^- entry as NKCC activity increased the $[Na^+]_i[K^+]_i[Cl^-]_i^2$ product. The increased Na^+–K^+-ATPase activity was primarily due to increased $[Na^+]$, and to a lesser degree to the depolarization of E_m and the reduction in $[K^+]_i$, this latter change occurring despite K^+ influx, due to the diluting effect of water influx. Thirdly, it must be noted that cessation of NKCC activity allowed complete and rapid recovery of E_m and V_c to their original set points.

Figure 9*B* shows the effect of NKCC activity in a cell with the $P_{Cl} : P_K$ ratio reduced from the approximately 3 : 1 ratio of skeletal muscle (Hodgkin & Horowicz, 1959) to a 0.05 : 1 ratio similar to that of, for example, erythrocytes (Freedman & Novak, 1997). All other parameters, including starting conditions and P_{NKCC} were identical to those in Fig. 9*A* to allow direct comparison of the interaction between NKCC and P_{Cl}. It is clear that P_{Cl} profoundly influences the possible consequences of NKCC activity. Firstly, the increase in V_c (> 40%) was very much greater in a cell with low P_{Cl}. Secondly, this significant swelling was accompanied by only a small depolarization of E_m (< 10% change). Thirdly, the rate of volume recovery following cessation of NKCC activity was very much slower, reflecting the much slower return of the accumulated Cl^-_i to a passive transmembrane distribution.

In addition, final stable intracellular ion concentrations were also changed considerably less than in the cell with high P_{Cl} during NKCC activity. This is because the cell with high P_{Cl} showed a high rate of ion influx through the NKCC even at the point of V_c and E_m stability due to the much greater Cl^- efflux through the background leak channels, and despite the resultant increase in Na^+–K^+-ATPase activity, intracellular ion concentrations were significantly perturbed. In contrast, in the low P_{Cl} cell, the rate of ion influx through the NKCC was eventually severely limited

by the sustained high $[Cl^-]_i$, and this allowed relatively normal levels of Na^+–K^+-ATPase activity to restore other ion concentrations to close to their usual values. An important consequence of this finding is that maintenance of volume stability during similar levels of NKCC activity would require much greater energy expenditure in a cell with high P_{Cl} than in one with low P_{Cl}.

The simulations of high P_{Cl} tissue thus fully reconstruct the experimental findings of Ferenczi *et al.* (2004) which showed that NKCC activity in skeletal muscle increased the volume of cells shrunken in hypertonic solutions only marginally, and instead depolarized cells sufficiently to compensate for the hyperpolarization otherwise seen in similarly treated muscle fibres in Cl^--free solutions (as Adrian, 1956), or in which the NKCC had been inhibited. It was therefore concluded that NKCC served to stabilize E_m in skeletal muscle in hypertonic solutions, and the current findings correspond well with this conclusion. The relative magnitudes of the influence upon V_c and E_m of cation–chloride cotransport in the high P_{Cl} simulation are close to those reported experimentally by Ferenczi *et al.* (2004). In each case, the magnitude of the influence upon E_m is 2–3 times the magnitude of the influence upon V_c. Similarly, in the low P_{Cl} simulation, the magnitude of the influence of NKCC activity upon E_m is $< 20\%$ of the magnitude of the change in V_c, compatible with the role of this transporter as a primarily volume regulatory mechanism in the majority of non-excitable tissues (Russell, 2000).

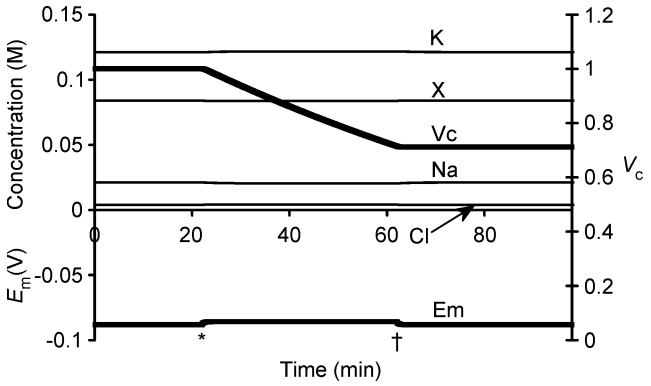

Figure 10. Organic osmolyte efflux
Organic osmolyte efflux was simulated by introducing a small membrane permeability to organic anions, $P_X = 0.0001$, at the point marked *, allowing gradual outward diffusion of X^-. Such efflux drove steady water efflux and volume reduction. It also caused a small depolarization from −89 mV to −86 mV, as would be expected from the introduction of a permeability term for an otherwise internally sequestered anion. In contrast to the effect of a similar period of cation–chloride cotransport (Fig. 9), the volume change was able to continue almost indefinitely without any further alteration to the membrane potential. Most strikingly, the cessation of organic osmolyte efflux (at the point marked †) showed that the volume reduction was not reversed by continued activity of the sodium pump, in sharp contrast to volume changes resulting from inorganic ion fluxes.

Finally, the effects of K^+–Cl^- cotransporter (KCC) activity ($P_{KCC} = 100$) were also investigated (Fig. 9*C*). Its activity resulted in a slight reduction in $[Cl^-]_i$, although its activity was clearly limited by the initially low $[Cl^-]_i$. However, although this precluded significant volume decrease by this mechanism, there was a small (∼5 mV) hyperpolarization of E_m. Higher or lower values of P_{KCC} (1000 or 10) produced very similar changes to V_c and E_m, reflecting the fact that activation of this transporter quickly equalizes the $[K^+]_i[Cl^-]_i$ and $[K^+]_e[Cl^-]_e$ products. Finally, V_c and E_m returned to their original values on cessation of KCC activity.

Organic anion fluxes result in significant and sustained changes to cell volume without causing sustained changes to E_m. Cation–chloride cotransport thus appeared unable to significantly change V_c in skeletal muscle due to the high P_{Cl}, and was unable to produce V_c changes that were sustained following cessation of cotransport activity, with the rate of recovery to resting V_c influenced by P_{Cl}. Instead, they caused significant, although similarly unsustained, changes to E_m, resulting primarily from the effect of changes to $[Cl^-]_i$.

In contrast, volume-sensitive organic anion fluxes have been implicated in the volume regulatory process in a variety of excitable tissues, including cardiac muscle (Rasmusson *et al.* 1993), barnacle muscle (Pena-Rasgado *et al.* 2001) and hippocampal neurones (Pasantes-Morales *et al.* 2000; Olson *et al.* 2003). Their contributions to volume and E_m regulation were accordingly investigated by introducing a term to the model reflecting a small permeability to X^-_i (P_X). Figure 10 demonstrates that introduction of $P_X = 0.0001$ resulted in gradual volume reduction accompanied by a small depolarization of E_m. However, in contrast to the effect of cation–chloride cotransport activity, this volume reduction could continue indefinitely, while E_m stabilized at this slightly depolarized value. Most significantly, reduction of P_X back to zero resulted in a return of E_m and all intracellular ionic concentrations to normal, but at a significantly reduced V_c. Furthermore, linkage of organic anion fluxes to cation fluxes (Schultz & Curran, 1970; Hudson & Schultz, 1984, 1988), using electroneutral cotransport models analogous to that used for the cation–chloride cotransporters, allowed volume decrease or increase without the transient E_m shift that resulted from organic anion flux alone (data not shown). However, at cessation of the activity of such transporters, the steady state values of V_c and E_m were determined solely by the magnitude of the change in X^-_i and z_X, and were not influenced by the accompanying cation flux. Finally, organic ion influx similarly resulted in sustained volume increase without E_m change (data not shown).

Organic anion fluxes therefore emerge as the sole mechanism by which muscle cells may change both V_c

and the V_c set point without simultaneously changing E_m. This is in marked contrast to every other mechanism by which V_c could be changed that was investigated in the current study, including cation–chloride cotransport activity, inorganic ion permeability or content changes, sodium pump density and changes to the mean valency of intracellular impermeant anions. Thus it seems likely that such fluxes could underlie volume change in short-term volume regulation as well as longer-term changes such as muscle growth, hypertrophy and atrophy. In contrast, cells with low P_{Cl} could employ cation–chloride cotransporters to cause volume changes, with little influence on E_m, although long-term changes to V_c or E_m set points may still require changes to the cellular content or mean valency of intracellular organic anions.

Discussion

This paper clarifies the quantitative relationships between two fundamental and related functional parameters, cell volume, V_c, and resting potential, E_m, and investigates the possible mechanisms for their determination, maintenance and regulation, particularly in excitable cells. It used a novel approach to calculate E_m directly from the intracellular charge difference, rather than using the Goldman-Hodgkin-Katz (GHK) equation or one of its more recent derivatives. It therefore represents the first quantitative analysis of the interdependence of V_c and E_m to calculate E_m using a method that does not require any assumption of steady state, permitting precise calculation of E_m even under non-equilibrium conditions. This approach was necessary because the steady state assumption ($dE_m/dt = 0$) that is central to the GHK equation and its derivatives precludes entirely accurate calculation of E_m and V_c in the same formalism, as this assumption is violated when V_c and hence E_m is changing. Earlier papers therefore separately considered E_m regulation in excitable cells such as skeletal muscle (Adrian, 1956; Hodgkin & Horowicz, 1959), and nerve (Hodgkin *et al.* 1952; reviews: Noble, 1966; Thomas, 1972) using the GHK approach, while V_c regulation was considered, again separately, in terms of electrolyte and organic solute fluxes in non-excitable cells (Tosteson & Hoffman, 1960; Schultz & Curran, 1970; Hudson & Schultz, 1984, 1988).

This analysis was made possible by the quantitative characterization now available about individual processes that might influence E_m and V_c. The present model thus incorporated all the known major steady state membrane permeabilities and transport processes, including electrogenic ion transport (Hernandez *et al.* 1989; Hernandez & Chifflet, 2000). It also incorporated identified membrane transport processes that are known to influence and/or respond to cell volume (review: Lang *et al.* 1998*b*) including cation–Cl^- cotransport (Lauf & Adragna, 2000; Russell, 2000) and changes in cation or anion permeability (Zhang *et al.* 1993; Nilius *et al.* 1996; Strange *et al.* 1996) or membrane capacitance (Huang, 1981*a*,*b*). Finally, the effects of organic anion fluxes (Rasmusson *et al.* 1993; Pasantes-Morales *et al.* 2000; Olson *et al.* 2003) were simulated explicitly through modelling of otherwise membrane-impermeant anions with non-unity valency.

This study was therefore able to show quantitatively, for the first time to our knowledge (O'Neill, 1999), that even in the absence of specific cellular mechanisms for volume detection, V_c converges to a fixed set point and that this is largely determined by the intracellular membrane-impermeant solute content (X^-_i) and its mean charge valency (z_X). Furthermore, for given sodium pump densities and sets of membrane ion permeabilities, E_m was shown to be determined *solely* by z_X. This approach thus provided straightforward demonstrations, for the first time to our knowledge, of a number of strategic properties of the *determination* of E_m and V_c in the reconstituted system. It was further shown that the charge-difference model introduced here was necessary to demonstrate these apparent set points, as they were not predicted by otherwise identical GHK- or Mullins-Noda-based models.

The principles of volume *regulation* were also investigated. The specific modelling examples were prompted by a number of both early and more recent experimental observations of manoeuvres designed to modify both E_m and V_c. First, early experiments demonstrated that under conditions where K^+ was the only significant membrane-permeant ion skeletal muscle V_c followed a simple inverse dependence upon extracellular osmolarity, while E_m followed the resultant K^+ Nernst potential (Adrian, 1956; Dydynska & Wilkie, 1963; Blinks, 1965). Subsequent studies demonstrated swelling-induced regulatory volume decreases (RVDs) (O'Neill, 1999; Okada *et al.* 2001) and shrinkage-induced regulatory volume increases (RVIs) brought about by cotransporter activity in many other, often non-excitable, cell types (reviews: Lang *et al.* 1998*a*; O'Neill, 1999). However, such regulatory volume adjustments have not been observed in mature skeletal muscle fibres (Sejersted & Sjogaard, 2000). Instead, recent findings have suggested a complex relationship between E_m and V_c that may vary between cell types. For example, a recent study reported that skeletal muscle fibres in Cl^--containing extracellular solutions did not hyperpolarize following osmotically induced shrinkage despite increased $[K^+]_i/[K^+]_e$ (Adrian, 1956). Ferenczi *et al.* (2004) demonstrated that in this situation Na^+–K^+–$2Cl^-$ cotransport (NKCC) held $[Cl^-]_i/[Cl^-]_e$ above equilibrium values but did not cause significant regulatory volume increases (RVIs) in agreement with earlier work (Blinks, 1965). Thus in skeletal muscle the volume-sensitive cation–chloride transport processes that underlie volume regulation in other cell types appeared instead to influence

Table 3. Summary of main findings for a cell with constant Na^+–K^+-ATPase density and ion permeabilities

In a cell with constant Na^+–K^+-ATPase density and ion permeabilities:

- The steady state volume (V_c) is determined by the total impermeant anion content (X^-_i) and its mean valency (z_X).
- The steady state membrane potential (E_m) and intracellular solute concentrations are determined by z_X alone.
- z_X *must* be significantly negative if a cell is to be highly polarized.
- The Na^+–K^+-ATPase is able to attain and maintain these steady-state values of V_c and E_m without extrinsic regulation of its activity.
- Cation-chloride cotransport activity may change V_c and E_m by altering the transmembrane Cl^- distribution.
- V_c and E_m recover to their set points following cessation of cation-chloride cotransport activity at a rate determined primarily by the Cl^- permeability (P_{Cl}).
- Sustained changes to the V_c set point that do not change E_m can only result from mechanisms that change X_i.
- When chloride is passively distributed, V_c and E_m are related as follows:

$$V_{c(t=\infty)} = \frac{(1 - z_X)[X^-]_{i(t=0)}}{(\Pi_e - 2[Cl^-]_e e^{(E_m F/RT)})}$$

E_m (Baumgarten & Clemo, 2003; Geukes Foppen, 2004) apparently in place of significant influences upon V_c (Ferenczi *et al.* 2004). However, while exercise increases muscle fibre volume by up to 20% (Sjogaard *et al.* 1985), long-term muscle fibre volumes *in vivo* remain remarkably stable (review: Proske & Morgan, 2001) despite the apparent short-term regulation of E_m in preference to V_c (Ferenczi *et al.* 2004). These discrepancies were explored in the present study, and mechanisms by which E_m and V_c may be regulated independently were identified.

The present study was therefore able to formulate several principles underlying volume determination and regulation. These principles are summarized in Table 3.

First, the CD model inherently converged to stable final values that closely reproduced *in vivo* intracellular ion concentrations and E_m. The latter additionally agreed precisely with the corresponding value calculated from these final ionic concentrations using the Mullins-Noda (MN) equation (Mullins & Noda, 1963). This convergence did not require any extrinsic modulation of Na^+–K^+-ATPase activity through either E_m or V_c. These steady state values were independent of initial intracellular inorganic ion concentrations, membrane capacitance, and any interposed perturbations given similar conditions of sodium pump density, ion permeabilities and intracellular impermeant osmolyte content. In contrast, simulations whose individual steps calculated E_m from the MN rather than the CD equation converged to significantly different $[Na^+]_i$, $[K^+]_i$, $[Cl^-]_i$ and $[X^-]_i$ and E_m values that were influenced by initial intracellular inorganic ion concentrations. However, the final ion concentrations contained large charge discrepancies reflecting accumulating errors from the inherent assumption that $dE_m/dt = 0$, and failed an analytic criterion constraining the relationship between steady state V_c and E_m for cells with passive transmembrane distributions of Cl^- (see Appendix).

Secondly, investigation of the relative importance of the sodium pump density (N) and transmembrane ion permeabilities in the determination of V_c and E_m demonstrated that even large variations in Na^+–K^+-ATPase activity above a critical value had little influence on V_c and E_m values. This is explicable in terms of a fixed pump stoichiometry that would define a point where the free energy output of hydrolysis of 1 molecule of ATP is insufficient to balance the free energy requirements of pumping 3 Na^+ and 2 K^+ against their respective electrochemical gradients (Jansen *et al.* 2003). Stepwise reductions in N from a high value had little influence on V_c or E_m until a critical value of N, below which V_c and E_m became unstable. Only when N was very close to this critical value could its value significantly influence V_c and E_m. Furthermore, changes in N could not independently influence V_c and E_m.

Thirdly, the critical value of N necessary to maintain stable values of V_c and E_m was determined primarily by the overall cation permeability. Proportional increases in both P_{Na} and P_K altered this critical value. Conversely, altering the magnitude of P_{Na}, P_K or N at a constant $P_{Na} : P_K : N$ proportion left the final stable values of V_c and E_m unchanged but produced a directly proportional change in the *rate* at which these stable values of V_c and E_m recovered from any given perturbation. In contrast, alterations in the $P_{Na} : P_K$ ratio influenced E_m (Hodgkin & Katz, 1949; Hodgkin & Horowicz, 1959), with an increase in this ratio resulting in depolarization at any given sodium pump density. Finally, P_{Cl} did not influence either the stable values of V_c or E_m, or the critical value of N for any non-zero value of P_{Cl}.

Fourthly, in contrast to the independence of V_c and E_m from initial intracellular inorganic ion concentrations, the simulations demonstrated that the intracellular membrane-impermeant solute content (X^-_i) and its mean charge valency (z_X) are the primary determinants of the steady state value of V_c. Thus given stable ion permeabilities and a fixed sodium pump density sufficient to attain a stable cell volume, cells with identical initial $[X^-]_i$ and z_X reached identical final stable values of E_m,

V_c, $[Na^+]_i$, $[K^+]_i$, $[Cl^-]_i$ and $[X^-]_i$ that were entirely independent of other starting conditions, including the initial values of E_m, $[Na^+]_i$, $[K^+]_i$ and $[Cl^-]_i$ and initial total intracellular osmolarity. Furthermore, use of accepted values of N (Clausen, 2003), P_{Na}, P_K and P_{Cl} (Adrian, 1956) gave final values of E_m, $[Na^+]_i$, $[K^+]_i$, $[Cl^-]_i$ and $[X^-]_i$ that were similar to those found in the literature (Maughan & Recchia, 1985) and independent of the initial values of any of the dependent variables and of membrane capacitance. However, while initial $[X^-]_i$ did not influence the final values of E_m, $[Na^+]_i$, $[K^+]_i$, $[Cl^-]_i$ and $[X^-]_i$, it profoundly influenced final cell volume.

In contrast, z_X influences the final stable values of E_m, $[Na^+]_i$, $[K^+]_i$, $[Cl^-]_i$, $[X^-]_i$ and V_c. It is thus the primary determinant of E_m, assuming constant ion permeabilities and sodium pump density. Thus more negative charge valencies resulted in larger, more polarized cells. Strikingly, the negative charge on X^-_i was shown to be an *absolute requirement* for significantly polarized values of E_m at any value of N. For example, at the $P_{Na} : P_K$ ratio of skeletal muscle the stable values of E_m were at least −85 mV for all values of $z_X > 1$, but if $z_X < 0.1$, the maximum polarization of E_m at any value of N was approximately −50 mV. If z_X is very low or zero, it is not possible to obtain the high intracellular $[K^+]_i$ necessary to produce polarized values of E_m, as clearly a similarly high concentration of some negatively charged ion is then required. The negative charge carried by X^-_i normally balances this charge on K^+_i, and Cl^- cannot perform a similar role, as it is excluded from a polarized cell.

Fifthly, the final simulations in the model suggested that separate mechanisms mediate transient and steady-state changes in V_c, particularly in skeletal muscle. Short-term volume regulatory mechanisms particularly involving volume-sensitive cation–chloride cotransport systems (Lauf & Adragna, 2000; Russell, 2000) or anion channels (Zhang *et al.* 1993; Nilius *et al.* 1996; Strange *et al.* 1996) have been reported in a wide range of cell types. Yet mature skeletal muscle does not perform RVI or RVD in response to applied osmotic stress (Sejersted & Sjogaard, 2000). Furthermore there is considerable evidence for the presence of the NKCC cotransporter in skeletal muscle and for its activation by cellular volume changes (Dorup & Clausen, 1996; Wong *et al.* 1999; Russell, 2000; Lindinger *et al.* 2002). Recent experimental evidence suggests that it may stabilize E_m following cell shrinkage rather than perform RVI (Ferenczi *et al.* 2004). The current study corroborates this suggestion by showing that the high membrane P_{Cl} of skeletal muscle precludes NKCC activity increasing V_c without also resulting in depolarization of E_m. Furthermore, ion fluxes through the NKCC decreased as they increased intracellular $[Cl^-]_i$, and such fluxes were opposed by increases in Na^+–K^+-ATPase activity secondary to increased $[Na^+]_i$ and depolarization of E_m. Therefore a new steady-state V_c and E_m could be reached despite continued NKCC activation. In cells with low P_{Cl}, such as erythrocytes (Tosteson & Hoffman, 1960), the simulations showed that an identical NKCC activation could increase V_c without greatly depolarizing E_m. Furthermore, the V_c at the new steady-state was considerably greater, and the increase in Na^+–K^+-ATPase activity considerably lower, than in the high P_{Cl} cell. Due to reduced passive re-equilibration of Cl^- in low P_{Cl} tissues, $[Cl^-]_i$ was greater at the new steady state, and this resulted in a greater opposition to ion influx through the NKCC. This in turn caused a lesser increase in Na^+ influx at steady state, when compared to that in high P_{Cl} tissues, and so provoked a lesser increase in Na^+–K^+-ATPase activity, and therefore less opposition to the NKCC-driven V_c increase.

The mechanism of RVD using the KCC, a method common to a number of cell types (Lang *et al.* 1998*a*; O'Neill, 1999), was also studied. One might expect its activity to be severely limited in excitable cells, simply because $[Cl^-]_i$ is extremely low in such highly polarized cells. However, the KCC is expressed in skeletal muscle (Lauf & Adragna, 2000), and the present simulations showed that KCC activity is energetically favoured in resting muscle, and that its activity, whilst unable to significantly alter cell volume, may be able to reduce $[Cl^-]_i/[Cl^-]_e$ below the ratio determined by passive distribution according to the membrane potential. Thus it was shown that KCC activity could potentially cause significant hyperpolarization in skeletal muscle, as due to the high P_{Cl} in this tissue a change in the equilibrium potential of Cl^- will be reflected by a changed E_m. Thus this cotransporter could potentially have a role in stabilizing muscle E_m, for example during exhaustive exercise.

It was shown that the V_c and E_m changes resulting from cation–chloride cotransport were entirely reversed on cessation of their activity, due to the action of the sodium pump. Again, this was principally true for muscle tissue: although Na^+–K^+-ATPase activity was shown eventually to restore cell V_c and E_m following any discrete perturbation of intracellular ionic content in a cell with any non-zero P_{Cl}, the rate at which it was able to do so was dependent on the P_{Cl} and therefore recovery was slow if P_{Cl} was low. In other words, high P_{Cl} was shown to assist the activity of the sodium pump in restoring normal intracellular ionic concentrations, V_c and E_m following a perturbation of any of their values, and likewise a low P_{Cl} significantly hampered it. It is interesting to speculate whether this constitutes a part of the physiological significance for the high P_{Cl} in skeletal muscle (Adrian, 1956), reflecting the high and unpredictable levels of activity in this tissue.

This influence of P_{Cl} is also of wider interest in view of the broad range of tissues in which volume-sensitive Cl^- channels have been identified (review: Nilius *et al.*

1996). It is clear that P_{Cl} can have no influence on V_c or E_m if its transmembrane distribution is entirely passive. This study has shown, however, that P_{Cl} influences the rate at which a cell attains its set volume. Therefore any change in the set volume, such as would follow organic ion fluxes, would result in a more rapid cellular volume change if P_{Cl} was simultaneously increased, thereby facilitating re-equilibration of Cl^-_i.

Finally, a mechanism by which excitable cells, and skeletal muscle in particular, may be able to regulate volume without simultaneously changing E_m was identified. The efflux of organic anions was shown to result in volume decrease limited only by the initial cellular content of this class of osmolyte, and without the large changes in membrane potential resulting from cation–chloride fluxes. Indeed, volume-related organic ion fluxes have been identified in a number of excitable tissues including cardiac muscle (Rasmusson *et al.* 1993), barnacle muscle (Pena-Rasgado *et al.* 2001) and hippocampal neurones (Pasantes-Morales *et al.* 2000; Olson *et al.* 2003). In contrast, NKCC and KCC activity may, in certain tissues, regulate E_m and not cellular volume.

Appendix

The relationship between V_c, E_m, Π_e, X_i and z_X at steady state is constrained as follows:

(1) Intracellular and extracellular osmolarity must be equal:

$$[X^-]_i + [Na^+]_i + [K^+]_i + [Cl^-]_i = \Pi_e$$

(2) Total intracellular charge is almost exactly zero:

$$[Na^+]_i + [K^+]_i - [Cl^-]_i + z_X[X^-]_i \approx 0$$

(3) Substituting for $[Na^+]_i + [K^+]_i = [Cl^-]_i$ - $z_X[X^-]_i$

$$[X^-]_i - z_X[X^-]_i + 2[Cl^-]_i = \Pi_e$$

$$\text{Thus} [X^-]_i = (\Pi_e - 2[Cl^-]_i)/(1 - z_X)$$

(4) X^- is membrane impermeant, and thus any change to X^-_i (i.e. a transient change in $[X^-]_i$) drives transmembrane water fluxes until $[X^-]_i$ is restored to its original value (see Fig. 7). If $V_c = 1$ at $t = 0$, then at steady state:

$$V_{c(t=\infty)} = [X^-]_{i(t=0)}/[X^-]_{i(t=\infty)}$$

(5) Therefore the relationship between V_c, X^- and z_X is:

$$V_{c(t=\infty)} = \frac{(1 - z_X)[X^-]_{i(t=0)}}{(\Pi_e - 2[Cl^-]_i)}$$

(6) If Cl^- is passively distributed, then:

$$[Cl^-]_i = [Cl^-]_e e^{(E_m F/RT)}$$

(7) Therefore at steady state and under conditions of passive chloride distribution, the relationship between V_c and E_m is:

$$V_{c(t=\infty)} = \frac{(1 - z_X)[X^-]_{i(t=0)}}{(\Pi_e - 2[Cl^-]_e e^{(E_m F/RT)})}$$

This can also be expressed as:

$$V_{c(t=\infty)} = \frac{(1 - z_X)(X^-_i/V_{c(t=0)})}{(\Pi_e - 2[Cl^-]_e e^{(E_m F/RT)})}$$

References

Adrian RH (1956). The effect of internal and external potassium concentration on the membrane potential of frog muscle. *J Physiol* **133**, 631–658.

Aickin CC, Betz WJ & Harris GL (1989). Intracellular chloride and the mechanism for its accumulation in rat lumbrical muscle. *J Physiol* **411**, 437–455.

Armstrong CM (2003). The Na/K pump, Cl ion, and osmotic stabilization of cells. *Proc Natl Acad Sci U S A* **100**, 6257–6262.

Baumgarten CM & Clemo HF (2003). Swelling-activated chloride channels in cardiac physiology and pathophysiology. *Prog Biophys Mol Biol* **82**, 25–42.

Blinks JR (1965). Influence of osmotic strength on cross-section and volume of isolated single muscle fibres. *J Physiol* **177**, 42–57.

Clausen T (2003). Na^+-K^+ pump regulation and skeletal muscle contractility. *Physiol Rev* **83**, 1269–1324.

Dorup I & Clausen T (1996). Characterization of bumetanide-sensitive Na^+ and K^+ transport in rat skeletal muscle. *Acta Physiol Scand* **158**, 119–127.

Dydynska M & Wilkie DR (1963). The osmotic properties of striated muscle fibres in hypertonic solution. *J Physiol* **169**, 312–329.

Eisenberg RS & Gage PW (1969). Ionic conductances of the surface and transverse tubular membranes of frog sartorius fibers. *J General Physiol* **53**, 279–297.

Else PL, Windmill DJ & Markus V (1996). Molecular activity of sodium pumps in endotherms and ectotherms. *Am J Physiol Regul Integr Comp Physiol* **271**, R1287–R1294.

Ferenczi EA, Fraser JA, Chawla S, Skepper JN, Schwiening CJ & Huang CL-H (2004). Membrane potential stabilization in amphibian skeletal muscle fibres in hypertonic solutions. *J Physiol* **555**, 423–438.

Freedman JC & Novak TS (1997). Electrodiffusion, barrier, and gating analysis of DIDS-insensitive chloride conductance in human red blood cells treated with valinomycin or gramicidin. *J General Physiol* **109**, 201–216.

Frigeri A, Nicchia GP, Balena R, Nico B & Svelto M (2004). Aquaporins in skeletal muscle: reassessment of the functional role of aquaporin-4. *FASEB J* **18**, 905–907.

Gage PW & Eisenberg RS (1969). Capacitance of the surface and transverse tubular membrane of frog sartorius muscle fibers. *J General Physiol* **53**, 265–278.

Geukes Foppen RJ (2004). In skeletal muscle the relaxation of the resting membrane potential induced by K^+ permeability changes depends on Cl^- transport. *Pflugers Arch* **447**, 416–425.

Geukes Foppen RJ, Van Mil HGJ & Van Heukelom JS (2002). Effects of chloride transport on bistable behaviour of the membrane potential in mouse skeletal muscle. *J Physiol* **542**, 181–191.

Goldman DE (1943). Potential, impedance and rectification in membranes. *J General Physiol* **27**, 37–60.

Hernandez JA & Chifflet S (2000). Electrogenic properties of the sodium pump in a dynamic model of membrane transport. *J Membr Biol* **176**, 41–52.

Hernandez JA & Cristina E (1998). Modeling cell volume regulation in nonexcitable cells: the roles of the Na^+ pump and of cotransport systems. *Am J Physiol* **275**, C1067–C1080.

Hernandez J, Fischbarg J & Liebovitch LS (1989). Kinetic model of the effects of electrogenic enzymes on the membrane potential. *J Theor Biol* **137**, 113–125.

Hodgkin AL & Horowicz P (1959). The influence of potassium and chloride ions on the membrane potential of single muscle fibres. *J Physiol* **148**, 127–160.

Hodgkin AL, Huxley AF & Katz B (1952). Measurement of current-voltage relations in the membrane of the giant axon of Loligo. *J Physiol* **116**, 424–448.

Hodgkin AL & Katz B (1949). The effect of sodium ions on the electrical activity of the giant squid axon. *J Physiol* **108**, 37–77.

Huang CL-H (1981*a*). Dielectric components of charge movements in skeletal muscle. *J Physiol* **313**, 187–205.

Huang CL-H (1981*b*). Membrane capacitance in hyperpolarized muscle fibres. *J Physiol* **313**, 207–222.

Huang CL-H & Peachey LD (1989). Anatomical distribution of voltage-dependent membrane capacitance in frog skeletal muscle fibers. *J General Physiol* **93**, 565–584.

Hudson RL & Schultz SG (1984). Sodium-coupled sugar transport: effects on intracellular sodium activities and sodium-pump activity. *Science* **224**, 1237–1239.

Hudson RL & Schultz SG (1988). Sodium-coupled glycine uptake by Ehrlich ascites tumor cells results in an increase in cell volume and plasma membrane channel activities. *Proc Natl Acad Sci U S A* **85**, 279–283.

Jansen MA, Shen H, Zhang L, Wolkowicz PE & Balschi JA (2003). Energy requirements for the Na^+ gradient in the oxygenated isolated heart: effect of changing the free energy of ATP hydrolysis. *Am J Physiol Heart Circ Physiol* **285**, H2437–H2445.

Lang F, Busch GL, Ritter M, Volkl H, Waldegger S, Gulbins E & Haussinger D (1998*a*). Functional significance of cell volume regulatory mechanisms. *Physiol Rev* **78**, 247–306.

Lang F, Busch GL & Volkl H (1998*b*). The diversity of volume regulatory mechanisms. *Cell Physiol Biochem* **8**, 1–45.

Lauf PK & Adragna NC (2000). K-Cl cotransport: properties and molecular mechanism. *Cell Physiol Biochem* **10**, 341–354.

Lindinger MI, Hawke TJ, Lipskie SL, Schaefer HD & Vickery L (2002). K^+ transport and volume regulatory response by NKCC in resting rat hindlimb skeletal muscle. *Cell Physiol Biochem* **12**, 279–292.

Maughan DW & Godt RE (2001). Protein osmotic pressure and the state of water in frog myoplasm. *Biophys J* **80**, 435–442.

Maughan D & Recchia C (1985). Diffusible sodium, potassium, magnesium, calcium and phosphorus in frog skeletal muscle. *J Physiol* **368**, 545–563.

Mullins LJ & Noda K (1963). The influence of sodium-free solutions on the membrane potential of frog muscle fibers. *J General Physiol* **47**, 117–132.

Nilius B, Eggermont J, Voets T & Droogmans G (1996). Volume-activated Cl^- channels. *General Pharmacol* **27**, 1131–1140.

Noble D (1966). Applications of Hodgkin-Huxley equations to excitable tissues. *Physiol Rev* **46**, 1–50.

Okada Y, Maeno E, Shimizu T, Dezaki K, Wang J & Morishima S (2001). Receptor-mediated control of regulatory volume decrease (RVD) and apoptotic volume decrease (AVD). *J Physiol* **532**, 3–16.

Olson JE, Kreisman NR, Lim J, Hoffman-Kuczynski B, Schelble D & Leasure J (2003). Taurine and cellular volume regulation in the hippocampus. *Adv Exp Med Biol* **526**, 107–114.

O'Neill WC (1999). Physiological significance of volume-regulatory transporters. *Am J Physiol* **276**, C995–C1011.

Pasantes-Morales H, Franco R, Torres-Marquez ME, Hernandez-Fonseca K & Ortega A (2000). Amino acid osmolytes in regulatory volume decrease and isovolumetric regulation in brain cells: contribution and mechanisms. *Cell Physiol Biochem* **10**, 361–370.

Pena-Rasgado C, Pierce SK & Rasgado-Flores H (2001). Osmolytes responsible for volume reduction under isosmotic or hypoosmotic conditions in barnacle muscle cells. *Cell Mol Biol* **47**, 841–853.

Proske U & Morgan DL (2001). Muscle damage from eccentric exercise: mechanism, mechanical signs, adaptation and clinical applications. *J Physiol* **537**, 333–345.

Rasmusson RL, Davis DG & Lieberman M (1993). Amino acid loss during volume regulatory decrease in cultured chick heart cells. *Am J Physiol* **264**, C136–C145.

Russell JM (2000). Sodium-potassium-chloride cotransport. *Physiol Rev* **80**, 211–276.

Schultz SG & Curran PF (1970). Coupled transport of sodium and organic solutes. *Physiol Rev* **50**, 637–718.

Sejersted OM & Sjogaard G (2000). Dynamics and consequences of potassium shifts in skeletal muscle and heart during exercise. *Physiol Rev* **80**, 1411–1481.

Sjogaard G, Adams RP & Saltin B (1985). Water and ion shifts in skeletal muscle of humans with intense dynamic knee extension. *Am J Physiol* **248**, R190–R196.

Strange K, Emma F & Jackson PS (1996). Cellular and molecular physiology of volume-sensitive anion channels. *Am J Physiol* **270**, C711–C730.

Thomas RC (1972). Electrogenic sodium pump in nerve and muscle cells. *Physiol Rev* **52**, 563–594.

Thompson LV & Fitts RH (1992). Muscle fatigue in the frog semitendinosus: role of the high-energy phosphates and P_i. *Am J Physiol* **263**, C803–C809.

Tosteson DC & Hoffman JF (1960). Regulation of cell volume by active cation transport in high and low potassium sheep red cells. *J General Physiol* **44**, 169–194.

Verkman AS (1992). Water channels in cell membranes. *Annu Rev Physiol* **54**, 97–108.

Wong JA, Fu L, Schneider EG & Thomason DB (1999). Molecular and functional evidence for Na^+-K^+-$2Cl^-$ cotransporter expression in rat skeletal muscle. *Am J Physiol* **277**, R154–R161.

Zhang J, Rasmusson RL, Hall SK & Lieberman M (1993). A chloride current associated with swelling of cultured chick heart cells. *J Physiol* **472**, 801–820.

Acknowledgements

The authors thank the Medical Research Council for project (G9900365 and G0100188) and Co-operative Group Grants (G9900182 and G01001986, respectively), and the Wellcome Trust Joint Research Equipment Initiative (JREI: 055203/Z/98/Z/ST/RC) for equipment funding support. CLHH also thanks the Leverhulme Trust and the British Heart Foundation for support. J.A.F. holds a George Henry Lewes Studentship.